

Published in final edited form as:

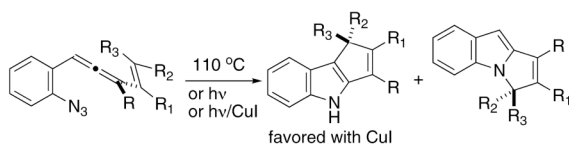
J Org Chem. 2009 July 17; 74(14): 4958–4974. doi:10.1021/jo900659w.

Allenyl Azide Cycloaddition Chemistry. 2,3-Cyclopentennelated Indole Synthesis through Indolidene Intermediates

 Ken S. Feldman^{*,†}, D. Keith Hester II[†], Malliga R. Iyer[†], Paul J. Munson[†], Carlos Silva López^{*,‡}, and Olalla Nieto Faza[‡]
[†]Department of Chemistry, The Pennsylvania State University, University Park, Pennsylvania 16802

[‡]Departamento de Química Organica, Universidade de Vigo, Lagoas Marcosende, 36200 Vigo, Galicia, Spain

Abstract



The thermal, photochemical, and photochemical/CuI-mediated cascade cyclizations of a range of substituted 1-(2-azidophenyl)-3-alkenylallenes are described. These reactions provide both 1,2- and 2,3-cyclopentennelated indole products in varying ratios. In most cases, high regioselectivity for the 2,3-annelated isomer can be achieved under the *hν*/CuI conditions. Computational studies of this multistep reaction support the intermediacy of indolidene intermediates whose electrocyclizations (with or without copper present) define the regioselectivity branch point in the sequence.

Introduction

Cascade cyclization sequences offer great promise for the expeditious assembly of polycyclic products. To the extent that these processes convert readily accessible cascade precursors to polycyclic products with predictable control of relevant selectivity issues (i.e., chemoselectivity, regioselectivity, stereoselectivity, enantioselectivity), these transformations may impact favorably on total synthesis efforts directed toward complex polycyclic natural products. It is within this context that the allenyl azide cascade cyclization sequence was developed, as the potential for accessing cyclopentennelated indole products from simple ortho-positioned (3-alkenyl)allene phenylazide substrates was apparent, Scheme 1. Preliminary results documented that species **1** under diverse reaction conditions rapidly and cleanly proceeded to the regioisomeric indole products **4a** and **4b**.^{1a} Furthermore, reaction conditions could be identified that led to high levels of regioselectivity for the C–C-bonded indole product **4a**.^{1b} Computational tools were brought to bear on this complex cascade sequence, and the initial mechanistic picture that emerged from these calculated models implicated indolidenes **3a** and **3b** as pivotal intermediates linking allenyl azide **1** to products

© 2009 American Chemical Society

ksf@chem.psu.edu; csilval@uvigo.es.

Supporting Information Available: General experimental procedures, copies of ¹H and ¹³C NMR spectra for **13i**, **14j**, **19–25**, **27c**, **28c**, **29**, **30**, **35c**, **37**, **38h,i,m**, **39n**, **40g**, **42a,f,g**, **43e**, **45e**, **46**, **47**, **58b**, and **59–61**, details of the X-ray crystallographic structural determinations of **39n**, **40a**, **42b,d**, **43e**, and **54**, 2-D energy profiles for the **64** → **67** conversion and its desmethyl lower homologue, and Cartesian coordinates and SCF energies of all of the computed structures. This material is available free of charge via the Internet at <http://pubs.acs.org>.

4a and **4b**.² In addition, these *in silico* models provided a rationale for the regioselectivity (or lack thereof in certain circumstances) observed.

Potential natural product targets for this developing methodology are plentiful, provided that both stereochemical and regiochemical requirements can be met by the allenyl azide cascade cyclization. For example, the Fisher indoles (cf. **5**),³ the indole diterpenes (cf. **6**),⁴ and the unique triindole yeast isolate malasseziacitrin (**7**)⁵ all fall under this general structural class, Scheme 2. Reaction chemistry that evolves from reactive indolidene intermediates of the type **3** has not been well described.⁶ One notable exception involves the proposed intermediacy of indolidene (or protonated indolidene) species in the syntheses of ibogaine derivatives and dimeric alkaloids of the vinblastine series, Scheme 2.⁷ The fact that this putative intermediate is reactive (electrophilic) enough to efficiently trap the sterically hindered and modestly nucleophilic aryl ring of vindoline suggests that further development of the reaction chemistry of indolidenes has the potential for advances in several areas of indole synthesis/functionalization.

In this full accounting of our work in this area, the scope of cyclopentennelated indole synthesis is investigated by examining several new allenyl azide substrates that probe the limits of the methodology. In addition, new calculational results that aid in elucidating mechanistic subtleties are presented; these calculations examine the “real system” and so extend beyond the model system calculations reported earlier.

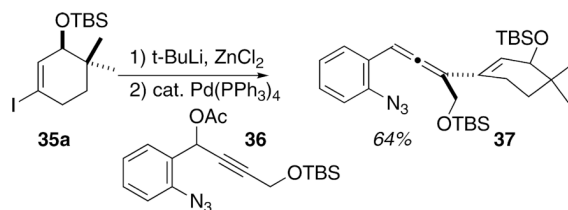
Results and Discussion

The exploratory studies commenced with the preparation of some simple 1-(2-azidophenyl)-3-alkenylallenes **13** and the analogous 1-(2-azidophenyl)-3-arylallenes **14**, Table 1. The propargylic acetate displacement chemistry of Krause proved completely serviceable in this task, using either commercially available zinc nucleophiles or zinc species generated *in situ* from the corresponding Grignard reagent and ZnCl₂.⁸ All of the allenyl azide substrates prepared in this study are racemic, and these species are a mixture of diastereomers when a second stereogenic element is present. The steric character of the substituent R directly attached to the allene was varied significantly (CH₃ → CH₂OTBS → Ph → TMS → t-Bu) in order to probe the consequences of steric bulk on the partitioning between **3a/3b** and/or **4a/4b**. As it transpired, an unexpected diversion of reactive intermediates with the R = TMS case (*vide infra*) limited the value of this entry in the steric comparison series. In this series of substrates, the 1-alkenyl position (i.e., R₁) was subjected to some variation also (H → CH₃ → Ph) with the expectation that R/R₁ clashes (cf. **3a/3b**) might also influence the regioselectivity profile of the reaction. The aryl series **14j–m** was designed to probe for electronic effects on product formation (yield, regioselectivity), but the route illustrated by the conversion of **12** (R = CH₃) into **14** did not afford products that survived attempts at chromatographic (SiO₂) purification. Therefore, the crude allenyl azides **14j–m** were subjected to thermal rearrangement without further purification. Subsequently, we determined that slightly modifying the sequence so that a methyl nucleophile was added to a phenyl-substituted propargyl acetate (**12j**, R = Ph) did furnish an allenyl azide **14j** that tolerated passage over SiO₂ and could be isolated as a pure, discrete compound. However, disappointing results upon thermolysis (*vide infra*, Scheme 5) did not encourage revisiting the syntheses of the other aryl substrates **14k–m**.

A related series of 1-(2-azidophenyl)-3-alkenylallenes **16** and **23–25** (Table 2 and Scheme 3, respectively) were prepared by slightly different routes than those described above. For the synthesis of **15**, a preformed alkenyl acetylide anion was employed to introduce the propargyl acetate functionality, and then methyl cuprate was utilized as the allene-forming nucleophile. The preparation of **23–25** featured a Sonogashira coupling of the preformed propargyl acetate

12i with the appropriate alkenyl iodide fragment **17–19** to deliver the enyne acetates **20–22**. The cuprate chemistry was relied upon again to deliver the allene product. These substrates introduced one (or two) substituents at the alkene terminus, a position destined to participate directly in C–C or C–N bond formation (cf. the red bonds in **4a/4b**). In this way, the influence of steric effects (primarily) and possibly electronic effects can be assessed upon attempted cyclopentenelated indole formation. The substrate **16b** in particular will test the premise that even very challenging all-carbon quaternary centers might be forged through this methodology.

A series of cyclohexenyl alcohol-based substrates were prepared in order to test the feasibility of accessing the tetracyclic skeleton of the Fisher indoles via this methodology (cf. **5**, Scheme 2, Table 3, and eq 1). The majority of these species were prepared by application of the chemistry developed for Scheme 3; Sonogashira coupling of **12i** with the requisite cyclohexenyl iodide **26** followed by alkyl cuprate-mediated propargylic displacement of the acetate function in **27** to deliver the allene product **28**. Since the cuprate required to prepare **37** (see eq 1) was not available, we resorted to the Krause chemistry with the highly functionalized cyclohexenyl zincate derived from **35a** and the propargyl acetate **36**, itself prepared from **11** and the TBS ether of propargyl alcohol. The various cyclohexenyl iodides **34** and **35a–c** were synthesized from the commercially available dione **31** using routine and well-documented chemistry, Scheme 4.⁹ The free hydroxyl substrate **29** was conveniently available by desilylation of **28a**. The ketone **30**, prepared via oxidation of **29**, was synthesized as well. The rationale behind the choice of these cyclohexenyl substrates was 2-fold; (1) the relationship between substrate structure and product regiochemistry was still underdeveloped at this early juncture of the research, and so probing the influence of allylic oxygen substitution (sterics, electronics?) on C–C vs C–N bond formation seemed appropriate, and (2) for the first time, the issue of relative stereochemistry, as is relevant to the C(10)/C(11) stereogenic centers in the Fisher indoles (cf. **5**, Scheme 2) can be addressed—how will the preexisting C(11) stereogenic center (–OR) influence the stereochemical outcome at C(10) upon C(3)/C(10) bond formation during electrocyclization of an indolidene species related to **3a**?



The initial attempts at cascade cyclization of the 1-(2-azidophenyl)-3-alkenylallenes followed the experimental protocol identified previously for the successful reaction of the simple saturated-linker 1-azido-3,4,6-heptatrienes.¹⁰ Those processes furnished cyclopentenelated dihydropyrrole products via an azatrimethylenemethane intermediate, and at the outset of this work, there was no reason, a priori, to expect that the phenyl-linked analogues would proceed through an alternative pathway. In fact, this argument-by-analogy proved to be mechanistically misleading (vide infra), although it led to satisfactory results in a practical sense. Specifically, heating a 100 mM toluene solution of the parent allenyl azide **13a** led efficiently to two new products in a 1.4:1 ratio following SiO₂ chromatography, Table 4. Spectroscopic analysis of the minor component left little doubt that an indole product **38a** was formed, presumably via formation of a C–C bond between C(3) and C(10) (Fisher indole numbering). However, the structure of the major product was a bit of a puzzle, as the methylene unit of this species appeared at a somewhat smaller value in the ¹H NMR spectrum (3.77 ppm) than expected for

the anticipated C–N cyclized product **39a**. Adding to the mystery was the observation that examination of the crude thermosylate by ^1H NMR spectroscopy did not reveal any of the signals for this compound; rather, a similar but still different species was present, with a methylene singlet at 4.53 ppm. The structure of this major isolated isomer tentatively was assigned as the pyrrole **40a** after comparison with the spectroscopic data from the desmethyl analogue of **40a**, a compound reported earlier by Kashulin and Nifant'ev¹¹ and later secured by single-crystal X-ray analysis (see the Supporting Information for details). It appears that the indole isomer **39a** was formed first as expected, but it suffered tautomerization to the pyrrole form **40a** upon exposure to SiO_2 . Thus, this index example offered the hope that the cyclization cascade might be developed into a high-yielding route to cyclopentennelated indoles (96% yield overall), but it also suggested that modifications were necessary in order to meet the goal of regioselective formation of the C–C-bonded isomer **38**.

One such modification might involve changing the size and/or electronic character of the substituents R , R_1 , and R_2 in the hope that steric discrimination in the transition states for bond formation might translate into regioselectivity. Toward that end, the size of the allene substituent “ R ” was increased from methyl (entry *a*) to $(\text{CH}_2)_2\text{OTBS}$ to *t*-Bu (entries *b* and *c*, respectively). Similar to the parent **13a**, thermolysis of the substrates **13b** and **13c** furnished products in high chemical yield. The regioselectivity did respond to these steric changes, with the preference for the C–C bonded isomer **38** increasing as the size of the R unit increased (1:1.4 for CH_3 to 1:1.2 for $(\text{CH}_2)_2\text{OTBS}$ to 2.9:1 for *t*-Bu). The regioselectivity for the related $R = \text{CH}_2\text{OTBS}$ case (entry *d*) was similar to the $R = \text{CH}_3$ case, but these results may be compromised by the overall lower yield.

Examination of steric effects at the R_1 site of **13** extended to just two compounds, $R_1 = \text{CH}_3$ and $R_1 = \text{Ph}$, entries *f* and *e*, respectively. Thermolysis of the $R_1 = \text{CH}_3$ compound **13f** furnished the two products **38f** and **40f** in equal proportions (Table 4, entry *f*). Enlarging R_1 to a phenyl substituent (Table 4, entry *e*) marginally increased the proportion of the C–C-bonded product **38e** upon thermolysis of **13e**. However, in neither case did the ratio of C–C to C–N bonded products vary significantly from the index case **13a** ($R_1 = \text{H}$). Thus, introducing steric bulk at the R_1 site had little effect. As a variation on this theme, the R and R_1 substituents were switched in entry *g* ($R = \text{Ph}$, $R_1 = \text{CH}_3$) in order to see if the same interaction (CH_3/Ph) when approached from the “other” direction had any different consequence. In fact, the C–C/C–N ratio (**38g**/**40g** = 1.2) upon thermolysis of **13g** fell in line with the earlier values of entry *e* (**38e**/**40e** = 1.3). Thus, there is no evidence to support the notion that a steric interaction between the R and R_1 substituents has any material influence on the overall regiochemistry of product formation.

Variation in the steric bulk at the R_2 position was expected to have the most profound effect on product regioselectivity since R_2 was right at the bond-forming site. This expectation was partially supported experimentally, as thermolysis of allenyl azide substrates with $R_2 = \text{CH}_2\text{OTBS}$ and $R_2 = \text{Ph}$ led to product regioisomer ratios that scarcely varied from 1:1, but when $R_2 =$ the larger TBS, the C–C bonded product was strongly favored (~ 5:1) over the C–N alternative. Note that the C–C-cyclized species **38j** did not survive SiO_2 chromatography, and so the reported yield derives from integration of characteristic signals in the ^1H NMR spectrum of the crude thermolysate. The *N*-cyclized species featured an indole unit **39** and not the previously observed pyrrole moiety of isomer **40**. Speculation about the absence of isomerization in this series might include the argument that planarization of the R_2 -bearing carbon upon pyrrole-forming isomerization would bring R_2 and the peri-positioned aryl hydrogen in conflict, a steric clash that is absent in the $R_2 = \text{H}$ substrates. The structural assignment of **39j** was confirmed by single crystal X-ray analysis of the derived hydrogenation product.^{1a} The lack of correlation between steric bulk at R_2 and regioselectivity of terminal bond formation was confounding at first, but a more thorough mechanistic analysis, guided by

density functional calculations, provided a consistent rationale by placing the regioselectivity-determining event earlier on the reaction coordinate than the final C–C (\rightarrow **38**) vs C–N (\rightarrow **39/40**) bond closures (vide infra).

Three disubstituted alkene substrates, **16c**, **16d**, and **24**, were examined in the thermolysis reaction in order to extend the scope of the transformation. The cyclic substrates **16c** (cyclopentenyl) and **16d** (cyclohexenyl) both participated in the cyclization cascade, but provided divergent types of products. The cyclohexenyl case (Table 4, entry *l*) delivered the expected C–C cyclized product **38l** and the isomerized C–N-cyclized regioisomer **40l** in a ratio slightly favoring the latter species. The cyclopentenyl substrate **16c**, on the other hand (Table 4, entry *k*), provided only the unisomerized C–N bonded indole product **39k** following SiO₂ chromatography. Signals characteristic of the tentatively assigned C–C bonded product **38k** could be detected in the ¹H NMR spectrum of the crude thermolysate in nearly equal amounts with **39k**, but this species did not survive the purification procedure. The differing stabilities of the similar tetracycles **38k** and **38l** to chromatography are surprising. Identifiable decomposition products from **38k** (or **38j**, another C-cyclized species intolerant to SiO₂) were not isolated, and so the basis for this sensitivity remains unknown. The final disubstituted alkene substrate **24** was subjected to thermolysis, leading to a preponderance of the sensitive N-cyclized product **40m** and only a trace of the C–C-bonded isomer **38m**.

A further extension of this alkene substitution theme led to the trisubstituted alkene analogue **16b**. This species was designed to test the premise that an all-carbon quaternary center might be accessible through this methodology. Thermally initiated cascade cyclization of **16b** proceeded in good yield to afford an approximately 2:1 ratio of the C–C/C–N-bonded products **38n** and **39n**, respectively. The structural assignment of the C–N-bonded isomer **39n** was based on single-crystal X-ray analysis (see the Supporting Information). Overall, the successful thermal cascade cyclization of the disubstituted alkene substrates **16c** and **16d** and the trisubstituted higher homologue **16b** do extend the scope of the methodology in potentially useful ways, but they do not lend any insight into the factors that might influence the key issue of regioselectivity upon terminal bond formation. In the final analysis, all of the efforts to probe the relationship between steric bulk and reaction regioselectivity for the three conceivable substrate variables R, R₁, and R₂ did not provide either promising results or even enough encouraging information to craft a useful model for further developing a substrate-based strategy to favor the formation of the C–C-bonded product **38** over the C–N-bonded alternative **39** (or **40**).

This discouraging state of affairs improved markedly when we turned to photochemistry to initiate the cascade process. Even then, however, success had to await one further chance discovery. The photochemistry experiments commenced without a clear notion of how light initiation might favorably influence the regiochemistry of the transformation, since a clear grasp of the mechanistic intricacies of the process still eluded us. Nevertheless, since ignorance should not tarnish hope, we proceeded to examine a few of the allenyl azide substrates under irradiation and found that, indeed, light at 254 nm did promote the cyclization cascade and furnish the expected suite of cyclopentennelated indole products (Table 4, entries *a–g*). However, no material improvement in the reaction regiochemistry followed from these examples—the usual unremarkable ratio of C–C **38** to C–N **39/40** bonded products were detected in yields comparable to the thermal cases. Thus, we learned that the sequence could be initiated with photons of appropriate energy, but it seemed likely that the same intermediate(s) were being accessed under either thermolysis or photolysis, led to the same nearly unbiased mixture of regioisomeric products.

During the course of these photolysis experiments, however, an unexpected observation was made. Every once in a while, a batch of allenyl azide substrate proceeded to indole product

with remarkably high regioselectivity (>10:1) favoring the C–C-cyclized product **38**. What distinguished these “exceptional” batches of substrate from the normal, disappointing ones? The key parameter was purity; the early nonregioselective runs utilized scrupulously purified and colorless allenyl azides that were obtained through careful SiO₂ chromatography even at the inevitable expense of material loss due to the sensitivity of these species. In some cases, however, batches of allenyl azide were obtained that had a light pink color despite appearing to be impurity-free by ¹H and ¹³C NMR spectroscopy. It was these colored batches that delivered indole product with high regioselectivity for the C–C-bonded isomer **38**. Once this connection was made, the search for the apparently critical “impurity” in the pink samples led to examination of test case photolysis reactions with substrate **28a** in the presence of various ingredients of the allenyl azide-forming reaction, which included CuI, LiBr, and Mg (see Table 5). Eventually, the key role of Cu(I) became apparent, and the salt CuI was chosen for its ready availability and solubility in the reaction solvent CH₃CN. Furthermore, it is mechanistically noteworthy that the improvement in regioselectivity scaled with the amount of CuI present. Reproducibly high regioselectivity favoring the C–C-bonded product **42b** was obtained when 150 mol % of CuI was included in the photolysis reaction mixture. None of the other additives tested, whether present in the allenyl azide synthesis or not, had any significant effect on the reaction regiochemistry. The role that copper plays in this complex process was still to be elucidated (vide infra), but this empirically derived solution to the regiochemical issue begged further study. In this light, reexamination of several of the allenyl azide substrates (Table 4) under the *hν*/CuI conditions led to favorable results overall, with a few notable exceptions. Simple unsubstituted-alkene substrates (Table 4, entries *a–d*) responded well to the new protocol, and the C–C-bonded regioisomer **38** was formed in good yield in ratios of at least 18:1 compared to the C–N-bonded isomer **40**. The monosubstituted-alkene substrates tested, **13e–g**, provided tricyclic indole product that appeared to consist exclusively of the C–C-bonded isomers **38e–g**, respectively. The C–N bonded products **40e–g** could not be detected in the ¹H NMR spectrum of the crude photolysate. The cyclohexenyl-substituted allenyl azide **16d** also provided only the C–C-bonded tetracycle **38l**. Two exceptions to this dramatic improvement in reaction regioselectivity can be seen in Table 4, entries *m* and *n*. Both the disubstituted alkene substrate **24** and the trisubstituted analogue **16b** did furnish good yields of tricyclic indole-containing products, but there was no apparent improvement in regioselectivity for **16b** over the thermally initiated case. Disubstituted alkene substrate **24** did proceed to indole product with an enhanced selectivity for the C–C-bonded isomer **38m** (C–C/C–N = 1:1) compared to the thermal case (C–C/C–N = 1:5), but the result was far short of the goal of strongly favoring the C–C-bonded isomer. Thus, it appears that these particular di- and trisubstituted alkene substrates can be induced to form indole products under the CuI/*hν* reaction conditions, but the high levels of regioselectivity for the C–C-bonded product experienced by simpler species do not translate for these entries.

The positive effect of copper inclusion on reaction regioselectivity in the photochemical series could be extended to the thermal chemistry as well, Table 5, entries *o–q*. Substrate concentration appeared to be a key variable, as a thermolysis experiment run at the photochemical experiment’s concentration of allenyl azide did not show any influence of the copper additive. Upon increasing the substrate concentration 10-fold, however, the copper effect became manifest; the C–C-bonded product **42b** was formed in a 5:1 ratio compared to the C–N-bonded isomer **43b** (Table 5, entry *q*). These concentration effects, and our suspicion that both photochemistry and thermal chemistry proceeded through common intermediates (vide supra), formed the basis of speculation on the role of copper in this transformation. This argument will be elaborated with the aid of density function calculations as discussed with Scheme 9 below.

The final series of allenyl azide substrates examined in this study featured functionalized cyclohexenyl rings as model systems for the Fisher indoles, Table 6. The structural variables

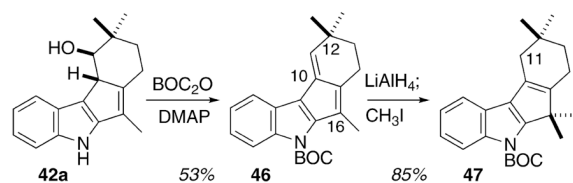
in this series included the allylic alcohol/ether substituent R, the carbinol group R₁, and the alkyl residue appended to C(3) of the allene, R₂. The reaction features that were tested by these structural probes comprised the overriding regioselectivity issue (C–C vs C–N terminal bond formation) and the relative stereochemistry emerging at C(10) under the influence of the adjacent C(11) stereogenic center. In addition, the sensitivity of the C(11) oxygen function to fulvene-forming elimination promoted by the potentially acidic C(10) cyclopentadiene proton was a concern. The preliminary CuI optimization studies with the OTBS variant **28a** detailed in Table 5 suggested that this latter issue might not arise as a general problem, as **42b** could be isolated without event following SiO₂ chromatography. The data displayed in Table 6 indicate that all of the cyclohexenyl alcohol derivatives **28a–e**, **29**, and **37** performed satisfactorily under the new *hν*/CuI conditions to deliver good yields of the C–C-cyclized products **42a–g**, respectively, accompanied by only trace amounts of the C–N-bonded regioisomer. The mildness of this protocol was evidenced by the functional group tolerance, which included a free alcohol, silyl ethers, and acid-sensitive alkyl ethers. The stereochemical outcome of all of the cyclizations examined was completely biased toward the C(10)/C(11) syn isomer shown as **42**; no evidence for minor species bearing an alternative stereochemistry was detected in the ¹H NMR spectrum of the crude photolysates. Surprisingly, even the cyanohydrin **42d**, whose structure was determined by single-crystal X-ray analysis (see the Supporting Information), did not deviate from this trend, perhaps because of the steric distinction between the OTBS and CN groups (A values: CN 0.15 kcal/mol (298 K, *t*-BuOH); ¹³a OSi(CH₃)₂-*t*-Bu 1.06 kcal/mol (179–188 K, CD₂Cl₂)¹³b–1.5 kcal/mol (193 K, CS₂ solvent).¹³c

In counterpoint, cyclohexenol-based allenyl azide cascade cyclizations performed under strictly thermal conditions afforded the usual mixture of the C–C- and C–N-cyclized regioisomers **42** and **43/44**, respectively, with little preference for one mode of cyclization over the other. Similarly, photochemistry without copper furnished indole products with nearly identical regioisomer ratios as in the thermal cases. These contrasting results emphasize the importance of copper(I) inclusion in the photolysis solution and are consistent with our preliminary interpretation that this metal salt plays a critical role in steering the partitioning of a reactive intermediate(s) between the two regioisomeric products.

The two substrates that included functionality on the allenyl methyl unit proceeded to indole products as expected, but not to the same type of indole products, which was unexpected (Table 6). The R₂ = TMS substrate **28e** was the outlier within this series. Reaction under thermal conditions did not afford any of the C–C-bonded indole product **42e**. Rather, the C–N-bonded regioisomer **43e** (X-ray analysis; see the Supporting Information) and a new type of product, the alkene **45**, predominated. ¹H NMR analysis of the crude thermolysate suggested that the first-formed alkene product actually had a TMS moiety on the indole nitrogen but that labile group suffers protodesilylation upon SiO₂ chromatography. The formation of this alkene can be rationalized by passage through an indolidene **3a** (cf. Scheme 1), which engages in silyl transfer in preference to C–C bond-forming electrocyclozation. Irradiation of **28e** sans copper did furnish evidence for the C–C-bonded indole product **42e** in the ¹H NMR spectrum of the crude product mixture, but the C–N-bonded regioisomer **43e** predominated. In the presence of copper(I), however, the photochemically derived product suite is entirely different, with the C–C-bonded regioisomeric indole **42e** largely favored and the C–N regioisomer **43e** absent. These observations provide further clues about the role of Cu(I) in influencing the regiochemical outcome of the cascade cyclization, a topic taken up in more detail below.

Using the Fisher indoles as a context for these studies introduces the need to convert sp²-hybridized C(16) of **42a** into a quaternary carbon bearing two methyl groups, eq 2. Toward this end, we discovered that hydride addition to an intermediate fulvene **46**, a species inadvertently derived from the alcohol **42a** upon *N*-BOC protection conditions, provided a

cyclopentadienylidene anion intermediate that methylates exclusively at C(16). This intermediate anion could, in principle, methylate at C(10) as well, but an incipient 1,3 diaxial interaction between the incoming methyl electrophile and the axial CH₃ of C(12) apparently thwarts this reaction trajectory. Of course, use of hydride as a nucleophile leaves C(11) in **47** devoid of functionality. Application of this methylation procedure in Fisher indole synthesis therefore will have to employ a nucleophilic species with fulvene **46** that preserves the opportunity to further functionalize C(11) as is required for **5**.



(2)

The TMS-substituted simple allenyl azide **13h** was examined with the expectation that an uneventful reaction would deliver products of the type **51a** and **52a**, Table 7. Less certain was the fate of the single allenyl-H-substituted system **13i**, given the propensity for H-substituted triazolines (cf. **2**, R = H) to tautomerize into stable aromatic triazoles.¹⁴ Whereas the standard indole products **51a/b** and **52a/b** were produced under certain circumstances, the big surprise with **13h** involved formation of the mechanistically informative triazoles **53** and **54**. The triazole **53** also was formed as a minor component from **13i**. The structural assignments of **51a/b**, **52a/b**, and **53** followed from their characteristic ¹H NMR data, but the structure of **54** remained a puzzle until single-crystal X-ray analysis revealed it to be the formal acetonitrile adduct shown (see the Supporting Information for details). Under thermolytic conditions with or without copper, the triazoles were the major species formed from **13h**. The formation of these compounds irrefutably implicates the intermediacy of a triazolone species **48a/b**, previously posited but otherwise unconfirmed. Apparently, the elevated temperature of these reaction conditions with **13h** provided enough energy for the nucleophilic capability of the allyl silane moiety within **48a** to be expressed; trapping by either adventitious protons or, remarkably, by acetonitrile, led to **53** and **54**, respectively. With **13i**, simple tautomerization within **48b**, presumably catalyzed by the same adventitious acid, delivers **53**. Irradiation of **13h** without copper(I) generates a reaction solution temperature of approximately 35 °C, and under this temperature regime the allyl silane moiety of **48a** participates only slightly in triazole formation. In this instance, the major products formed are the C–C- and C–N-bonded indoles **51a** and **52a**, respectively, in a ratio similar to that seen earlier with related substrates (Table 4). Copper-mediated photolysis of **13h** again produces a minor amount of the triazole **53**, but the major product is the C–C-bonded regioisomer **51a**, formed to the exclusion of the C–N-bonded alternative **52a**. The H-substituted substrate **13i** decomposed under irradiation and no further information was forthcoming from this species. The \pm CuI photochemistry of **13h** proceeded in a manner completely analogous to the other simple alkene-containing substrates. The anomalous behavior of the silyl-substituted substrate **13h** occurs at higher temperatures, where an alternative pathway involving electrophilic desilylation intervenes, and in so doing, preserves evidence for the intermediacy of the triazolone **48a**. Likewise, the thermal chemistry of **13i** argues for reaction through triazolone **48b**, but curiously, N₂ loss is competitive with tautomerization for this intermediate.

The final group of substrates examined feature an aryl substituent on the allenyl azide framework, **14j** – **14m**, Scheme 5. The challenge with this type of substrate lies in the competition within the indolide intermediates **55a/55b** between ^{1,7} H-shift and

electrocyclization through the aryl ring. Whereas the H-shift has always been a potentially problematic side-reaction, the electrocyclization through an *alkene* partner apparently won out energetically in all of the previous cases. With **14j** – **14m**, however, breaching the aromaticity of the aryl group evidently is not competitive, and only the [1,7] H-shift products **57j** – **57m** are formed in modest yields. Photochemistry with and without CuI present was explored with **14j**, although no evidence for redirection of the reaction course was detected. Thus, irradiation (254 nm) of **14j** in CH₃CN afforded only **57j** in 56% yield, whereas similar reaction in the presence of 1.5 equivalents of CuI provided this same product in 41% yield.

Finally, a discussion of the scope of the cascade cyclization would not be complete without acknowledging the 1-(2-azidophenyl)-3-alkenyl allene substrates that, for various reasons, did not participate productively in the transformation. For example, attempts to prepare a terminally disubstituted alkene substrate **62** were derailed by the facility of a 6 π -electron electrocyclization that affords the naphthalene product **61** following tautomerization within **63** (Scheme 6). This example can be contrasted with the successful formation and unexceptional cascade cyclization of the triphenylalkenyl allenyl azide substrate **16b**. A rationale for the lack of similar electrocyclization with this (*Z*)-phenyl-containing alkene might be traced to the additional phenyl group at position R₁ (cf. **16b**, Table 4), which might prevent access to the approximately planar conformation of the triene that should facilitate electrocyclization. Thus, the conformational consequences of the R/R₁ steric interaction (= CH₃/Ph in **16b**, but only = H/CH₃ in **62**) may be the decisive factor in both the stability and the successful reaction of **16b** and the failure of same with **62**. A second irretrievable failure attended the attempted cascade cyclization of the enone **30** (cf. Table 3). Under any conditions examined (thermal, photochemistry, photochemistry with CuI), this substrate was consumed quickly without formation of any characterizable products. Presumably, the electronic activation conferred by the carbonyl functionality introduced lower energy competitive pathways that drained away allenyl azide faster than the desired [3 + 2] cycloaddition process.

Mechanistic Analysis

The accumulated experimental evidence to date can be framed within a unified mechanistic scenario featuring a sequence of discrete triazoline and then indolidene intermediates as hypothesized in Scheme 1. However, many subtleties remain unresolved in this crude picture; for example, (a) which step is the slow step? (b) is loss of N₂ from the triazoline **2** concerted or stepwise? (c) what is the relationship between substituent R in **2** and the alkene geometry in **3a/3b**?, (d) what is the relationship between the alkene geometry of **3a/3b** and the regiochemistry of terminal bond formation, C–C (\rightarrow **4a**) or C–N (\rightarrow **4b**)?, and finally, (e) what is the role of Cu(I) in redirecting the regiochemistry of bond formation to strongly favor **4a**? In order to gain more insight into the details of this complex process and address these questions, we turned to density functional theory in its Kohn–Sham formulation, using the B3LYP/6–311+G(d,p)//B3LYP/6–31G(d,p) computational approach.¹⁵ Second derivatives of the energy with respect to the Cartesian nuclear coordinates were computed for all stationary points and subsequent harmonic analysis confirmed the nature (minimum or transition state) of each structure. Unscaled frequency values obtained from the second derivatives were employed for thermochemical analysis. The calculated reaction profile for the noncopper mediated thermal conversion of allenyl azide **13a** into the precursor **66** of the C–C bonded indole product **38a** and the precursor **39a** of the observed C–N bonded regioisomer **40a** is detailed in Scheme 7.

Interpretation of the energy values displayed on this reaction coordinate diagram provides an entry point for answering the mechanistic questions listed above. In order: (a) The rate-determining step appears to be the initial [3 + 2] cycloaddition to form triazoline **64**. (b) The conversion of triazoline **64** into the indolidenes **65a** and **65b** can, in principle, occur through

either concerted or stepwise loss of N₂. The calculated barriers for concerted N₂ loss, 16.5 kcal/mol for **65a** and 16.7 kcal/mol for **65b**, are likely to be smaller than the barrier for stepwise N₂ loss, although a transition state for the conversion of triazoline **64** into the singlet diyl **67** could not be located by this computational approach (see the Supporting Information for details). This claim may seem surprising at first glance, since the concerted loss of N₂ from **64** is equivalent to a formal suprafacial 12π-electron cycloreversion, a process that falls into the “forbidden” regime of the Woodward–Hoffmann (W–H) rules.¹⁶ How can these calculated results be reconciled with the otherwise infallibility of the W–H dogma? The key to understanding this apparent exception is appreciating the orthogonal relationship between the two π-systems (the indole and the N₂). From this perspective, as the C–N and N–N bonds stretch during the approach to the transition state, the two π systems scarcely “communicate” and there is no appreciable passage of electron density between them. This supposition is supported by the results of ancillary ACID¹⁷ and NICS¹⁸ calculations of N₂ loss from the desmethyl version of **64**.² These computational techniques provide “measurements” of electron density in off-atom regions of space, such as the region between the cleaving atoms in the transition state for N₂ extrusion. These calculations clearly indicate that almost no electron density occupies this key locale in the transition state for N₂ extrusion.² It appears that as the C–N bond stretches in **64**, the remaining N–N bond begins to stretch before the transition state to **67** is reached, and, in what might be characterized as a non-least-motion process, C(16) (cf. **64**) begins to rotate until the planarity of **65a/65b** is achieved. Overall, this N₂ loss process appears to be accidentally concerted, and the lack of electronic communication between the two components removes it from the W–H regime of cycloadditions.

The relationship between indolidene alkene geometry and substituent R (question (c)) is illustrated in Scheme 8. The direction of rotation about the indicated bond in **69** determines the eventual alkene geometry; rotation in direction *A* as shown leads to the (*E*)-isomer **70a**, whereas the alternative, rotation in direction *B*, delivers the (*Z*)-isomer **70b**. These rotational directions engender different steric interactions between the proximate substituents, and it is reasonable to suppose that the energetic trade-offs between these interactions ultimately determine the alkene geometry ratio. Rotational direction *A* increases the vinyl//H clash but relieves the R//H interaction, whereas rotational direction *B* has the opposite effect. To the extent that the substituent R is larger than a vinyl group, rotation away from the R//H interaction as in **69** (rotation *A*) would be expected to be favored, leading to preferred formation of **70a** over **70b**. The limited series of substrates **13a–c** (R = CH₃, (CH₂)₂OTBS, t-Bu, respectively) provide results consistent with this analysis. As the R substituent increases in size, the C–C bonded product emerging from **70a** is increasingly preferred; R = CH₃ 1:1.4 **38a/40a**, R = (CH₂)₂OTBS 1:1.2 **38b/40b**, and R = t-Bu 2.9:1 **38c/40c** (A values: CH₃ = 1.7 kcal/mol, ethyl = 1.75 kcal/mol, vinyl = 1.35 kcal/mol, t-Bu ≈ 4 kcal/mol).^{13a} DFT calculations largely support these conclusions. Thus, the calculated ratio of **65a/65b** derived from **13a** (R = CH₃, R₁ = H) is 55:45, a value that is not too dissimilar to the experimental ratio (42:58) of eventual isolable products **38a:40a** (Table 4, entry *a*). The calculated/experimental values for the analogous *tert*-butyl case **13c** (Table 4, entry *c*), remarkably, are completely coincident; 74:26 for **38c/40c**. Finally, calculations of the barriers for **65a/65b** formation from **13g** (R = Ph, R₁ = CH₃) predict a 90:10 ratio of C- to N-cyclized material; the experimental ratio of **38g/40g** is 55:45. The basis for this discrepancy has not been identified.

The importance of the alkene geometry of **65a** and **65b** on eventual product regiochemistry (question (d)) is highlighted as a result of these calculations. Each alkene isomer can proceed via an electrocyclization to give indole products, **65a** → **66** and **65b** → **39a**, though concerted processes that require surmounting activation barriers of only 14.5 kcal/mol for each transformation. In contrast, the barrier for interconversion of these alkene isomers is much higher; 33.2 kcal/mol, and so a non-Curtin–Hammett situation arises in which **65a** and **65b** lead directly to product without equilibration. Thus, these calculations provide numerical support

for a reactivity model in which the ultimate product regioisomer ratio (**4a/4b**, Scheme 1) replicates the indolidene alkene isomer population, which in turn reflects the differential steric interactions illustrated in Scheme 8.

The introduction of Cu(I) into this complex reaction sequence (question (e)) could, in principle, impact the chemistry at several different stages, Scheme 9. For example, the copper might play a defining role in the initial azide chemistry by forming a copper nitrene-type intermediate **74** by analogy with much prior copper-mediated amination chemistry.¹⁹ Alternatively, the copper might become involved in a much more passive capacity by providing a Lewis acidic binding site for various nitrogen donor ligands, as suggested by **71a/b**. Initially, the nature of the Cu(I) ligation was explored through calculation. An assumption underlying all of the Cu–ligand models examined for Cu solvation was made; the Γ^- was dissociated in the polar CH_3CN solvent, and so the active species was a version of $\text{Cu(I)}^+(\text{CH}_3\text{CN})_n$. From $n = 0$ up to three coordinated HCN molecules (as a model for the CH_3CN solvent used in the reactions) were explored computationally with several of the putative intermediates illustrated in Scheme 9. The structures and energies of species with no coordinating ligands (“naked copper(I)”) reflected the extreme electrophilicity of the metal, which was an unrealistic attribute for catalytic activity. Tricoordinated Cu(I) appeared to be too sterically hindered to participate in any productive interactions with the organic compounds present. Little energy difference was found between di- and monocoordinated copper with select intermediates of Scheme 9, but the singly coordinated $\text{Cu(I)}\cdot\text{HCN}$ complex consistently provided species with slightly lower energies, and so that motif was adopted for the calculational approach as a whole.

The initial question of importance focuses on the competition between copper-mediated nitrene **74** formation and orthodox [3 + 2] cycloaddition (\rightarrow **64**) within **13a** to start the cascade cyclization off. The calculated activation barriers are similar, with a slight edge going to the nitrene mechanism. The subsequent electrocyclization of **74** and reductive elimination within the Cu(III) species **75** are essentially barrierless processes by these calculations. Since the numerical values for the two distinct pathways from **13a** are within computational error, there is no basis to exclude either from further consideration. In fact, both starting points lead to the same intermediates, the Cu(I)-bound indolidenes **71a** and **71b**. The nitrene-based mechanism delivers these key species directly, whereas the [3 + 2] cycloaddition route requires a bimolecular step, Cu(I) ligation (not explicitly shown in Scheme 9; barrierless by these calculations), after the indolidenes **65a/65b** are formed by the previously discussed N_2 extrusion reaction. In neither chemistry is there yet any reason to link copper participation to a change in the regiochemistry of indole formation, the pivotal issue of this discussion.

The link between copper mediation and reaction regiochemistry comes at the next stage of the sequence, during which the indolidenes **71a** and **71b** electrocyclize to product tricycles **72** and **73**, respectively. The inclusion of Cu(I) in this part of the transformation perturbs the system in two profound ways: (1) The barrier to electrocyclization to form the C–N bonded species (**71b** \rightarrow **73**) is now significantly raised compared to the noncopper case of Scheme 7 (24.9 kcal/mol for **71b** vs 14.5 kcal/mol for **65b**). (2) The barrier to interconversion between the two indolidenes is now lower than the same barrier in the copper-free case (23.5 kcal/mol for **71a** \rightarrow **71b**, compared to 33.4 kcal/mol for **65a** \rightarrow **65b**). The barrier to C–C bond forming electrocyclization (**71a** \rightarrow **72**) remains largely unchanged by copper ligation (12.5 kcal/mol vs 14.5 kcal/mol for **65a** \rightarrow **66**). The confluence of these energy changes has significant consequences for the regioselectivity of the reaction. With Cu(I) present, the fate of the pre-C–N forming indolidene **71b** is now different than its fate with Cu absent. In the former instance, isomerization of **71b** to the pre-C–C bond forming indolidene **71a** is calculated to be faster than electrocyclization to afford **73**. Since the barrier to electrocyclization of **71a** is largely unperturbed by copper, its closure is now the fastest option available to this (*Z*)-indolidene. Thus, in contradistinction to the noncopper-mediated chemistry of Scheme 7, a

Curtin–Hammett situation appears to be at hand here; **71b** interconverts to its geometrical isomer **71a** faster than it proceeds to indole product **73**, while **71a** forms tricyclic product **72** faster than it returns to **71b**. The sum of these factors then favors formation of the C–C bonded product **72**. Thus, these calculations suggest that copper(I) inclusion in the cascade cyclization reaction may have two effects: (1) redirecting indolidene formation through a copper–nitrene intermediate and (2) ligating to, and retarding the rate of, electrocyclization of the pre-C–N bond forming indolidene. It is only this latter effect that influences reaction regioselectivity to favor the C–C bonded product **4a**. The two substrates **16b** and **24**, whose regiochemistry upon photocyclization did not benefit from CuI incorporation, may have suffered from unfavorable steric interactions between the alkene substituents and Cu(L)_n that mitigated against formation of the pivotal complex **71a**.

The cascade cyclizations of 1-(2-azidophenyl)-3-alkenylallenes provide 2,3-annelated indole-containing products under a range of experimental conditions. These transformations likely commence through initial [3 + 2] cycloaddition of the azide to the allene and then proceed through loss of nitrogen gas and electrocyclization of the derived indolidene. Computational studies of the energy surface for this complex transformation suggest that the central issue of C–C vs C–N regiochemistry of ultimate bond formation appears to be related to the differences in the activation energies for indolidene alkene isomer interconversion compared with the barriers for final C–C or C–N bond-forming electrocyclization. Incorporation of a nitrogen binding metal (CuI) can influence these energetic tradeoffs and in favorable cases steer the reaction toward high levels of C–C-bonded cyclopentannelated indole product. One family of substrates bearing functionalized cyclohexene rings as the “alkene” portion were particularly suitable for C–C bond forming cyclization, and the derived tetracyclic structures may find use in the synthesis of cognate natural products such as the Fisher indoles, *inter alia*.

Experimental Section

Computational Methodology

All of the stationary points were located with the B3LYP²⁰ density functional as implemented in Gaussian03²¹ in conjunction with the 6–31G(d,p) basis set. To further improve the electronic energy values, an energy refinement was computed with the larger triple- ζ quality 6–311+G(d,p) basis set. This scheme usually is noted as B3LYP/6–311+G(d,p)//B3LYP/6–32G(d,p).

Due to the potential diradical character of some of the structures considered in this work, the internal and external stability of the wave functions was computed via the Hermitian stability matrices **A** and **B** in all cases.²² For all of the structures exhibiting unstable restricted wave functions, the spin symmetry constraint of the wave function was released (i.e., expanding the SCF calculation to an unrestricted space, UB3LYP), leading to stable unrestricted wave functions.

This methodology has been tested extensively and compared against very robust and specialized methodology (CASSCF, CASPR2) for the study of oxa and aza derivatives of the trimethylenemethane motif.²³

General Procedure 1. Allenyl Azide Formation

To a solution of ZnCl₂ (2.5 equiv) in THF (0.3 M solution) was added the appropriate Grignard reagent (2.5 equiv), and the mixture was stirred at room temperature for 1 h. Pd(PPh₃)₄ (5 mol %) and the propargylic acetate (1 equiv) in THF (0.1 M solution) were added sequentially. The reaction mixture was allowed to stir at room temperature for 20 min (monitored by TLC for starting material consumption). After addition of an equal volume of a saturated NH₄Cl solution, the organic layer was extracted into Et₂O and washed with water and brine, dried over Na₂SO₄, and evaporated under reduced pressure maintaining a water bath temperature

below 40 °C. The resulting oil was purified by flash chromatography (hexanes → 2% Et₂O/hexanes).

General Procedure 2. Sonagashira Coupling

To a 0.5 M solution of alkenyl iodide in THF were added PdCl₂(PPh₃)₂ (10 mol %), 1-(2-azidophenyl)prop-2-ynyl acetate (**12i**) (1.6 equiv), Et₃N (7 equiv), and CuI (3 mol %). The mixture was stirred at room temperature under a nitrogen atmosphere for 16 h unless otherwise noted. The reaction solution was then diluted with an equivalent volume of Et₂O, and an equivalent volume of saturated NH₄Cl solution was added. The organic layer was washed (3 × H₂O, 3 × brine), dried over MgSO₄, and evaporated under reduced pressure. The resulting oil was purified by flash chromatography (1% Et₂O/hexanes → 15% Et₂O/hexanes).

General Procedure 3. Allenyl Azide Formation

CH₃MgBr (3.0 M in Et₂O, 10 equiv) was added dropwise to an ice-cold 0.1 M solution of CuI (10 equiv) and LiBr (10 equiv) in THF, and the resulting solution was stirred at that temperature for 30 min. A solution of the alkynyl azide in THF (0.1 M) was added slowly via cannula. The ice-cold solution was stirred for 30 min (monitored by TLC for starting material consumption). Ice-cold saturated NH₄Cl solution was then added dropwise until gas evolution ceased, and then the reaction mixture was diluted with an equivalent volume of Et₂O. The organic layer was washed (3 × ice-cold H₂O, 3 × ice-cold brine), dried over MgSO₄ and evaporated under reduced pressure maintaining a water bath temperature below 40 °C. The resulting oil was purified by flash chromatography (hexanes → 2% Et₂O/hexanes).

General Procedure 4. Copper-Mediated Photolysis of Allenyl Azides

A flame-dried quartz vessel containing a 5 mM solution of allenyl azide and 1.5 equiv of CuI in CH₃CN was vigorously purged with N₂ or Ar for 5 min. The vessel was irradiated at the specified wavelength for a minimum of 1 h with monitoring by TLC for starting material consumption. The reaction solution was diluted with an equivalent volume of Et₂O and washed 2× with ice-cold 10% NH₄OH in saturated NH₄Cl (1:4), 3× with ice-cold H₂O (until the aqueous phase exhibited pH = 7), and 3× with brine, dried over Na₂SO₄, and evaporated under reduced pressure. An alternative aqueous workup also was found to be effective: ice-cold 1 M Na₂S₂O₃, 2 × ice-cold 1 N H₃PO₄, 3 × ice-cold H₂O, and 3 × ice-cold brine. The residue was purified by flash chromatography (2% Et₂O/hexanes → 10% Et₂O/hexanes).

General Procedure 5. Thermolysis of Allenyl Azides

A flame-dried round-bottomed flask or sealed tube containing a 0.1 M solution of allenyl azide in toluene was refluxed for a minimum of 30 min under a N₂ atmosphere with monitoring by TLC for starting material consumption. The solvent was evaporated under reduced pressure and the residue was purified by flash chromatography (2% Et₂O/hexanes → 10% Et₂O/hexanes).

General Procedure 6. Photolysis of Allenyl Azides

A flame-dried quartz vessel containing a 5 mM solution of allenyl azide in CH₃CN was vigorously purged with N₂ or Ar for 5 min. The vessel was irradiated at the specified wavelength for a minimum of 1 h with monitoring by TLC for starting material consumption. The reaction solution was diluted with an equivalent volume of Et₂O, washed 3× with ice-cold H₂O and 3× with brine, dried over Na₂SO₄, and evaporated under reduced pressure. The residue was purified by flash chromatography (2% Et₂O/hexanes → 10% Et₂O/hexanes).

1-Azido-2-(4-methylpenta-1,2,4-trienyl)benzene (13i)

Following general procedure 1, isopropenylmagnesium bromide (0.5 M in THF, 4.6 mL, 2.3 mmol) and acetate **12i** (200 mg, 0.929 mmol) produced 90 mg (49%) of **13i** as a yellow oil: IR (neat) 2123, 1925 cm^{-1} ; ^1H NMR (400 MHz, CDCl_3) δ 7.40 (dd, $J = 7.8, 1.5$ Hz, 1H), 7.24 (td, $J = 7.7, 1.5$ Hz, 1H), 7.13 (dd, $J = 8.0, 1.1$ Hz, 1H), 7.08 (td, $J = 7.5, 1.1$ Hz, 1H), 6.70 (d, $J = 6.4$ Hz, 1H), 6.34 (d, $J = 6.5$ Hz, 1H), 5.02 (d, $J = 0.6$ Hz, 1H), 4.93 (q, $J = 1.5$ Hz, 1H), 1.82 (t, $J = 0.6$ Hz, 3H); ^{13}C NMR (100 MHz, CDCl_3) δ 208.5, 138.5, 136.3, 128.2, 128.1, 125.5, 124.9, 118.4, 114.6, 101.5, 91.8, 19.7; EI+ m/z (relative intensity) 169.1 (M - N_2 , 70%); HRMS (EI+) calcd for $\text{C}_{12}\text{H}_{11}\text{N}$ 169.0891, found 169.0973.

1-Azido-2-(3-phenylbuta-1,2-dienyl)benzene (14j)

Following general procedure 3, 400 mg (1.37 mmol) of acetate **12j** produced 275 mg (81%) of **14j** as a yellow oil: IR (neat) 2122, 1931 cm^{-1} ; ^1H NMR (300 MHz, CDCl_3) δ 7.36–7.33 (m, 2H), 7.31 (dd, $J = 8.5, 0.7$ Hz, 1H), 7.25–7.20 (m, 2H), 7.15–7.10 (m, 2H), 7.03 (ddd, $J = 8.1, 1.3, 0.4$ Hz, 1H), 6.96–6.91 (m, 1H), 6.65 (q, $J = 2.9$ Hz, 1H), 2.12 (d, $J = 3.0$ Hz, 3H); ^{13}C NMR (75 MHz, CDCl_3) δ 207.5, 136.4, 136.1, 128.4, 128.2, 128.1, 127.0, 125.80, 125.77, 124.8, 118.5, 104.5, 91.0, 16.7; ES+ m/z (relative intensity) 220.2 (M - N_2 + H, 20), 248.1 (M + H, 10); HRMS calcd for $\text{C}_{16}\text{H}_{14}\text{N}$ 220.1126, found 220.1122.

***tert*-Butyl-(2-iodovinyl)dimethylsilane (19)**

To an ice-cold stirring solution of $\text{Zr}(\text{Cp})_2\text{Cl}_2$ (1.82 g, 6.22 mmol) in 20 mL of THF was added DIBAL-H (1.0 M in hexanes, 6.22 mL, 6.22 mmol). The reaction was stirred at that temperature for 30 min, and then a solution of (*tert*-butyldimethylsilyl)acetylene (1.06 mL, 5.66 mmol) in 3 mL of THF was added slowly and the reaction allowed to warm to room temperature. Upon warming, the reaction mixture turned green and then red. The reaction solution was cooled to -78 $^\circ\text{C}$, a solution of I_2 (1.87 g, 7.36 mmol) in 5 mL of THF was added slowly, and stirring was continued at that temperature for 1 h. The reaction solution was then allowed to warm to room temperature, stirring was continued for 2.5 h, ice-cold 1 M HCl (35 mL) was slowly added, and the mixture was diluted with Et_2O (50 mL). The organic layer was washed with 1 M HCl (50 mL), 1 M $\text{Na}_2\text{S}_2\text{O}_3$ solution (2 \times 50 mL), saturated NaHCO_3 solution (50 mL), H_2O (3 \times 50 mL), and brine (3 \times 50 mL), dried over MgSO_4 , and concentrated under reduced pressure. The residue was purified by flash chromatography (hexanes) to provide 1.14 g (75%) of **19** as a pale yellow oil: ^1H NMR (360 MHz, CDCl_3) δ 7.04 (d, $J = 16.1$ Hz, 1H), 6.65 (d, $J = 16.2$ Hz, 1H), 0.86 (s, 9H), 0.02 (s, 6H); ^{13}C NMR (90 MHz, CDCl_3) δ 147.6, 90.1, 26.2, 16.6, -6.3 ; EI+ m/z (relative intensity) 141.1 (M - I, 20), 210.9 (M - *t*-Bu, 100), 268.0 (M⁺, 20); HRMS (EI+) calcd for $\text{C}_8\text{H}_{17}\text{SiI}$ 268.0144, found 268.0146.

Acetic Acid 1-(2-Azidophenyl)-6-(*tert*-butyldimethylsilyloxy)hex-4-en-2-ynyl Ester (20)

Following general procedure 2, with a reaction time of 4 h, 2.40 g (11.2 mmol) of **12i** and 2.08 g (6.97 mmol) of *tert*-butyldimethylsilyl-(*E*)-3-iodo-2-propenyl ether (**17**)²⁴ produced 1.99 g (74%) of **20** as a yellow oil: IR (neat) 2127, 1747 cm^{-1} ; ^1H NMR (300 MHz, CDCl_3) δ 7.66 (dd, $J = 7.6, 1.6$ Hz, 1H), 7.37 (td, $J = 7.7, 1.6$ Hz, 1H), 7.17 (m, 2H), 6.73 (d, $J = 1.8$ Hz, 1H), 6.25 (dt, $J = 15.8, 4.1$ Hz, 1H), 5.79 (dq, $J = 15.8, 2.2$ Hz, 1H), 4.20 (ddd, $J = 4.0, 2.2, 0.4$ Hz, 1H), 2.07 (s, 3H), 0.89 (s, 9H), 0.03 (s, 6H); ^{13}C NMR (75 MHz, CDCl_3) δ 169.3, 143.9, 137.7, 130.1, 129.2, 128.1, 124.9, 118.2, 107.5, 85.3, 85.0, 62.6, 61.2, 25.7, 20.9, 18.2, -5.5 ; ES+ m/z (relative intensity) 408.1 (M + Na, 100); HRMS (ES+) calcd for $\text{C}_{20}\text{H}_{27}\text{N}_3\text{O}_3\text{NaSi}$ 408.1719, found 408.1729.

Acetic Acid 1-(2-Azidophenyl)-7-(*tert*-butyldimethylsilyloxy)-4-methylhept-4-en-2-ynyl Ester (21)

Following general procedure 2, 605 mg (2.81 mmol) of alkyne **12i** and 573 mg (1.76 mmol) of iodide **18**²⁴ produced 514 mg (71%) of **21** as a yellow oil: IR (neat) 2126, 1747 cm⁻¹; ¹H NMR (360 MHz, CDCl₃) δ 7.66 (d, *J* = 7.6 Hz, 1H), 7.34 (td, *J* = 7.7, 1.4 Hz, 1H), 7.17–7.10 (m, 2H), 6.72 (s, 1H), 5.90 (t, *J* = 7.2 Hz, 1H), 3.59 (t, *J* = 6.8 Hz, 2H), 2.28 (app q, *J* = 6.9 Hz, 2H), 2.05 (s, 3H), 1.77 (s, 3H), 0.86 (s, 9H), 0.02 (s, 6H); ¹³C NMR (90 MHz, CDCl₃) δ 169.2, 137.7, 135.8, 130.0, 129.3, 128.3, 124.8, 118.3, 118.1, 89.8, 81.6, 61.9, 61.2, 32.2, 25.8, 20.8, 18.2, 17.0, -5.5; ES+ *m/z* (relative intensity) 436.3 (M + Na, 100); HRMS (ES+) calcd for C₂₂H₃₁N₃O₃SiNa 436.2032, found 436.2029.

Acetic Acid 1-(2-Azidophenyl)-5-(*tert*-butyldimethylsilyl)-pent-4-en-2-ynyl Ester (22)

Following general procedure 2, using 20 mol % of PdCl₂(PPh₃)₂, 1.14 g (4.25 mmol) of iodide **19**, and 1.46 g (6.80 mmol) of alkyne **12i** produced 332 mg (22%) of **22** as a yellow oil: IR (neat) 2127, 1746 cm⁻¹; ¹H NMR (360 MHz, CDCl₃) δ 7.67 (dd, *J* = 7.6, 1.4 Hz, 1H), 7.37 (td, *J* = 7.8, 1.5 Hz, 1H), 7.19–7.13 (m, 2H), 6.75 (d, *J* = 1.7 Hz, 1H), 6.50 (d, *J* = 19.4 Hz, 1H), 5.98 (dd, *J* = 19.3, 1.8 Hz, 1H), 2.08 (s, 3H), 0.86 (s, 9H), 0.01 (s, 6H); ¹³C NMR (90 MHz, CDCl₃) δ 169.3, 144.9, 137.7, 130.2, 129.2, 128.0, 124.9, 123.5, 118.2, 87.0, 85.1, 61.2, 26.3, 20.9, 16.5, -6.5; ES+ *m/z* (relative intensity) 295.1 (M - TBS + MeOH + Na, 100), 378.2 (M + Na, 10); HRMS (ES+) calcd for C₁₄H₁₄N₃O₃Na 295.0933, found 295.0941.

[6-(2-Azidophenyl)-4-methylhexa-2,4,5-trienyloxy]-*tert*-butyldimethylsilane (23)

Following general procedure 3, 263 mg (0.682 mmol) of acetate **20** produced 167 mg (72%) of **23** as a yellow oil: IR (neat) 2123, 1929 cm⁻¹; ¹H NMR (400 MHz, CDCl₃) δ 7.35 (dd, *J* = 7.7, 1.4 Hz, 1H), 7.24 (td, *J* = 7.2, 1.3 Hz, 1H), 7.13 (dd, *J* = 8.0, 1.0 Hz, 1H), 7.08 (td, *J* = 7.6, 1.0 Hz, 1H), 6.53 (s, 1H), 6.28 (dd, *J* = 15.6, 0.7 Hz, 1H), 5.78 (dtd, *J* = 15.6, 5.3, 1.2 Hz, 1H), 4.31 (t, *J* = 1.4 Hz, 1H), 4.29 (t, *J* = 1.4 Hz, 1H), 1.96 (s, 3H), 0.95 (s, 9H), 0.12 (s, 6H); ¹³C NMR (100 MHz, CDCl₃) δ 209.7, 136.3, 128.9, 128.4, 128.0, 127.3, 126.0, 124.8, 118.4, 103.3, 88.6, 63.9, 25.9, 18.4, 15.3, -5.2; ES+ *m/z* (relative intensity) 314.2 (M - N₂ + H, 80%); HRMS (AP+) calcd for C₁₉H₂₈NOSi: 314.1940, found 314.1936.

[7-(2-Azido-phenyl)-4,5-dimethyl-hepta-3,5,6-trienyloxy]-*tert*-butyl-dimethyl-silane (24)

Following general procedure 3, 512 mg (1.24 mmol) of acetate **21** produced 368 mg (80%) of **24** as a red oil: IR (neat): 2122, 1929 cm⁻¹; ¹H NMR (360 MHz, CDCl₃) δ 7.31 (dd, *J* = 7.7, 1.4 Hz, 1H), 7.17 (td, *J* = 7.6, 1.2 Hz, 1H), 7.07 (dd, *J* = 7.6, 1.2 Hz, 1H), 7.02 (t, *J* = 7.5 Hz, 1H), 6.54 (s, 1H), 5.50 (t, *J* = 7.2 Hz, 1H), 3.66 (t, *J* = 6.9 Hz, 2H), 2.37 (app q, *J* = 6.9 Hz, 2H), 1.94 (d, *J* = 2.6 Hz, 3H), 1.75 (s, 3H), 0.89 (s, 9H), 0.06 (s, 6H); ¹³C NMR (90 MHz, CDCl₃) δ 207.9, 136.1, 132.3, 128.0, 127.7, 126.6, 124.7, 122.6, 118.3, 107.6, 89.8, 62.7, 32.4, 25.9, 18.3, 16.2, 15.2, -5.3; ES+ *m/z* (relative intensity) 342.2 (M - N₂ + H, 100%), 387.3 (M + NH₄, 60%), 392.2 (M + Na, 30%); HRMS (ES+) calcd for C₂₁H₃₅N₄OSi: 387.2580, found 387.2578.

[5-(2-Azido-phenyl)-3-methyl-penta-1,3,4-trienyl]-*tert*-butyl-dimethyl-silane (25)

Following general procedure 3, 66 mg (0.19 mmol) of acetate **22** produced 34 mg (59%) of **25** as a yellow oil: IR (neat): 2121, 1929 cm⁻¹; ¹H NMR (400 MHz, CDCl₃) δ 7.31 (d, *J* = 7.6 Hz, 1H), 7.22 (t, *J* = 7.7 Hz, 1H), 7.11 (d, *J* = 7.9 Hz, 1H), 7.06 (t, *J* = 7.3 Hz, 1H), 6.54 (d, *J* = 18.9 Hz, 1H), 6.51 (s, 1H), 5.84 (d, *J* = 19.0 Hz, 1H), 1.91 (d, *J* = 2.5 Hz, 1H), 0.88 (s, 9H), 0.04 (s, 6H); ¹³C NMR (75 MHz, CDCl₃) δ 210.8, 142.3, 136.3, 128.5, 128.0, 126.8, 125.9, 124.8, 118.4, 105.4, 88.6, 26.4, 16.7, 14.6, -6.0, -6.1; ES+ *m/z* (relative intensity) 283.2 (M - N₂, 50%).

1-Azido-2-{3-[3-(tert-butyl-dimethyl-silyloxy)-4,4-dimethyl-cyclohex-1-enyl]-4-trimethylsilyl-but-1,2-dienyl}-benzene (28e)

Following general procedure 3 using TMSCH₂MgCl (1.0 M in Et₂O), 115 mg (0.251 mmol) of **27e** produced 115 mg (95%) of **28e** as a yellow oil: IR (neat): 2123, 1919 cm⁻¹; ¹H NMR (300 MHz, C₆D₆) δ 7.45 (m, 1H), 6.81 (m, 3H), 6.71 (m, 1H), 5.68 (d, *J* = 1.2 Hz, 1H), 3.96 (s, 1H), 2.25 - 2.10 (m, 2H), 1.75 (m, 2H), 1.43 (m, 1H), 1.31 (m, 1H), 1.00 (s, 9H), 0.96 (m, 3H), 0.94 (s, 3H), 0.15 (m, 3H), 0.10 (s, 12H); ¹³C NMR (75 MHz, CDCl₃) δ 208.1, 207.9, 136.2, 133.2, 133.0, 128.0, 127.7, 127.6, 127.5, 126.7, 124.8, 124.7, 118.4, 108.21, 108.18, 90.71, 90.65, 75.8, 75.7, 34.3, 34.23, 34.18, 34.1, 27.72, 27.66, 25.9, 24.9, 19.9, 19.7, 18.2, 18.1, 17.6, -0.8, -4.2, -4.9; APCI+ *m/z* (relative intensity) 454.3 (M + H - N₂, 100%), 482.3 (M + H, 15%); HRMS (AP+) calcd for C₂₇H₄₄NOSi₂: 454.2961, found 454.2979.

3-[3-(2-Azido-phenyl)-1-methyl-propa-1,2-dienyl]-6,6-dimethyl-cyclohex-2-enol (29)

To a 0 °C stirring solution of **28a** (429 mg, 1.05 mmol) in 10 mL of THF was added n-Bu₄NF (1.0 M in THF, 10 mL, 10 mmol). The reaction mixture was stirred at 0 °C for 54 h (monitored by TLC for starting material consumption). Ice-cold saturated NaHCO₃ solution (10 mL) was added and then the reaction mixture was diluted with Et₂O (10 mL). The organic layer was washed (ice-cold brine × 2), dried over Na₂SO₄ and evaporated under reduced pressure maintaining a water bath temperature below 40 °C. The resulting oil was purified by flash chromatography (neutral alumina, 25% EtOAc/hexanes) to give 289 mg (93%) of **29** as an orange oil: IR (neat): 3393, 2124, 1930 cm⁻¹; ¹H NMR (400 MHz, CDCl₃) δ 7.31 (m, 1H), 7.21 (m, 1H), 7.11 (dd, *J* = 8.0, 0.9 Hz, 1H), 7.05 (t, *J* = 7.8 Hz, 1H), 6.57 (s, 1H), 5.68 (m, 1H), 3.89 (d, *J* = 7.9 Hz, 1H), 2.11 - 2.03 (m, 2H), 1.96 (d, *J* = 2.7 Hz, 3H), 1.73 (br s, 1H), 1.50 (m, 1H), 1.39 (m, 1H), 0.96 (m, 3H), 0.90 (m, 3H); ¹³C NMR (100 MHz, CDCl₃) δ 207.9, 207.8, 136.11, 136.09, 135.1, 135.0, 127.93, 127.91, 126.1, 125.0, 124.8, 124.7, 118.4, 105.6, 90.2, 74.9, 74.6, 33.6, 33.5, 33.3, 32.9, 26.5, 26.2, 24.6, 24.5, 21.2, 20.7, 15.9; ES+ *m/z* (relative intensity) 318.1 (M + Na, 100%), 296.2 (M + H, 10%); HRMS (ES+) calcd for C₁₈H₂₁N₃ONa: 318.1582, found 318.1585.

3-[3-(2-Azido-phenyl)-1-methyl-propa-1,2-dienyl]-6,6-dimethyl-cyclohex-2-enone (30)

To a stirring solution of alcohol **29** (57 mg, 0.20 mmol) in 1 mL of CH₂Cl₂ was added a solution of Dess-Martin periodinane (170 mg, 0.40 mmol) in 2 mL of CH₂Cl₂ and the reaction was stirred for 1 min. Saturated NaHCO₃ (3 mL) was added and the organic layer washed with H₂O (3 × 5 mL), and brine (3 × 5 mL), dried over MgSO₄ and concentrated under reduced pressure. The residue was purified by flash chromatography (5% EtOAc/hexanes) to provide 24 mg (41%) of **30** as a yellow oil: IR (neat): 2124, 1927, 1664 cm⁻¹; ¹H NMR (360 MHz, C₆D₆) δ 7.21 (dd, *J* = 7.3, 1.7 Hz, 1H), 6.84 - 6.76 (m, 2H), 6.70 - 6.66 (m, 2H), 6.07 (d, *J* = 1.1 Hz, 1H), 2.20 (app pent, *J* = 6.1 Hz, 2H), 1.68 (d, *J* = 2.7 Hz, 3H), 1.46 (t, *J* = 6.2 Hz, 2H), 1.06 (s, 3H), 1.04 (s, 3H); ¹³C NMR (90 MHz, C₆D₆) δ 210.4, 202.7, 153.5, 136.9, 129.0, 128.4, 125.2, 124.9, 123.3, 118.9, 106.4, 91.5, 40.6, 36.4, 24.9, 24.3, 15.5; ES+ *m/z* (relative intensity) 316.1 (M + Na, 100%); HRMS (ES+) calcd for C₁₈H₁₉N₃ONa: 316.1426, found 316.1429.

[2-(3-Iodo-6,6-dimethyl-cyclohex-2-enyloxymethoxy)-ethyl]-trimethylsilane (35c)

To a stirring solution of alcohol **33** (355 mg, 1.41 mmol) in 5 mL of CH₂Cl₂ was added Bu₄NI (624 mg, 1.69 mmol), *N,N*-diisopropylethylamine (dried over Na₂SO₄ and decolorized with charcoal) (279 μL, 1.69 mmol), and SEMCl (tech. grade, 499 μL, 2.82 mmol). The reaction mixture was stirred for 16 h and then the solvent was removed in vacuo. The resulting oil was dissolved in Et₂O (10 mL) and washed (3 × 10 mL H₂O, 3 × 10 mL brine), dried over MgSO₄, and then the solvent was removed in vacuo. The resulting oil was purified by flash chromatography (hexanes → 10% Et₂O/hexanes) to yield 515 mg (96%) of **35c** as a colorless

oil: IR (neat): 1635 cm^{-1} ; ^1H NMR (360 MHz, C_6D_6) δ 6.45 (m, 1H), 4.57 (d, $J = 7.0$ Hz, 1H), 4.47 (d, $J = 7.0$ Hz, 1H), 3.66 - 3.56 (m, 2H), 3.46 (m, 1H), 2.28 (m, 2H), 1.28 (m, 1H), 1.06 (m, 1H), 0.91 (m, 5H), 0.77 (s, 3H), -0.02 (m, 9H); ^{13}C NMR (90 MHz, C_6D_6) δ 138.8, 99.3, 94.6, 81.4, 65.2, 37.7, 35.9, 32.8, 26.3, 21.8, 18.2, -1.2; EI+ m/z (relative intensity) 309.0 (M - SiMe_3 , 40%); HRMS (EI+) calcd for $\text{C}_{11}\text{H}_{18}\text{O}_2\text{I}$: 309.0352, found 309.0360.

1-Azido-2-{4-(tert-butyl-dimethyl-silyloxy)-3-[3-(tert-butyl-dimethyl-silyloxy)-4,4-dimethyl-cyclohex-1-enyl]-buta-1,2-dienyl}-benzene (37)

To a -78 °C solution of iodide **35a** (2.078 g, 8.243 mmol, 2.5 equiv) in 82 mL of THF was added dropwise *t*-BuLi (1.7 M in pentane, 10.7 mL, 18.1 mmol, 5.5 equiv) and stirring continued at that temperature for 30 min, during which time the solution turned deep yellow. A solution of ZnCl_2 (1.124 g, 8.243 mmol, 2.5 equiv) in 40 mL of THF was then added slowly and the resulting solution warmed to room temperature during which time the solution turned colorless. $\text{Pd}(\text{PPh}_3)_4$ (190 mg, 0.165 mmol, 5 mol %) and a solution of acetate **36** (1.185 g, 3.297 mmol, 1 equiv) in 33 mL of THF were added sequentially and the reaction mixture was stirred for 45 min (as monitored by TLC). Ice-cold saturated NH_4Cl solution (30 mL) was added slowly and the organic layer was diluted with Et_2O (30 mL). The organic layer was washed with H_2O (3×30 mL) and brine (3×30 mL), dried over MgSO_4 and concentrated in vacuo. The residue was purified by flash chromatography (2% Et_2O /hexanes) to produce 1.132 g (64%) of **37** as a yellow oil: IR (neat): 2123, 1929 cm^{-1} ; ^1H NMR (360 MHz, C_6D_6) δ 7.41 - 7.49 (m, 1H), 6.85 (d, $J = 5.8$ Hz, 1H), 6.78 - 6.81 (m, 2H), 6.65 - 6.68 (m, 1H), 5.96 (s, 1H), 4.49 - 4.60 (m, 2H), 3.96 (s, 1H), 2.02 - 2.15 (m, 2H), 1.44 - 1.49 (m, 1H), 1.28 - 1.34 (m, 2H), 1.01 (m, 9H), 0.98 (s, 3H), 0.93 - 0.97 (m, 11H), 0.18 (s, 3H), 0.10 (s, 3H), 0.07 (m, 6H); ^{13}C NMR (90 MHz, C_6D_6) δ 208.1, 208.0, 136.7, 136.6, 131.4, 131.3, 128.5, 128.40, 128.35, 128.1, 126.2, 126.1, 125.03, 124.95, 118.71, 118.67, 111.6, 92.54, 92.49, 76.0, 75.8, 62.7, 62.6, 34.4, 34.3, 34.0, 33.9, 27.7, 27.5, 26.2, 26.0, 25.4, 25.3, 20.8, 20.5, 18.4, -3.7, -4.6, -5.0, -5.1; ES+ m/z (relative intensity) 512.3 (M + H, 35%), 562.3 (M + Na, 100%); HRMS (ES+) calcd for $\text{C}_{30}\text{H}_{49}\text{N}_3\text{O}_2\text{Si}_2\text{Na}$: 562.3261, found 562.3242.

2-Methyl-1-phenyl-8H-3a-aza-cyclopenta[a]indene (40g)

Method A: Following General Procedure 4, 48 mg (0.18 mmol) of **13g** provided 30 mg (69%) of **38g**^{1b} as a yellow oil. Method B: Following General Procedure 5, 193 mg (0.71 mmol) of **13g** provided 81 mg (47%) of **38g**^{1b} as a yellow oil and 67 mg (39%) of **40g** as a white solid. Method C: Following General Procedure 6, 100 mg (0.37 mmol) of **13g** provided 21 mg (23%) of **38g**^{1b} as a yellow oil. **40g**: mp. 89 - 90 °C; ^1H NMR (400 MHz, CDCl_3) δ 7.40 (m, 2H), 7.31 (m, 2H), 7.26 (d, $J = 7.4$ Hz, 1H), 7.19 - 7.11 (m, 2H), 7.08 (d, $J = 7.7$ Hz, 1H), 6.95 (t, $J = 7.3$ Hz, 1H), 6.87 (s, 1H), 3.84 (s, 2H), 2.23 (s, 3H); ^{13}C NMR (100 MHz, CDCl_3) δ 140.9, 136.2, 133.8, 132.9, 128.4, 127.5, 127.4, 125.7, 125.2, 122.7, 122.1, 117.5, 109.2, 109.1, 29.7, 12.6; ES+ m/z (relative intensity) 246.1 (M + H, 100%); HRMS (ES+) calcd for $\text{C}_{18}\text{H}_{16}\text{N}$: 246.1283, found 246.1286.

1-(tert-Butyl-dimethyl-silyloxymethyl)-3-methyl-1,4-dihydro-cyclopenta[b]indole (38 h) and 3-(tert-Butyl-dimethyl-silyloxymethyl)-1-methyl-3H-3a-aza-cyclopenta[a]indene (39 h)

Following General procedure 5, 95 mg (0.28 mmol) of **23** produced 21 mg of **38h** (24%) and 30 mg of **39h** (34%). **38h**: (yellow oil): IR (neat): 3401 cm^{-1} ; ^1H NMR (400 MHz, C_6D_6) δ 7.81 (d, $J = 7.4$ Hz, 1H), 7.26 (t, $J = 7.0$ Hz, 1H), 7.21 (m, 2H), 6.73 (br s, 1H), 6.28 (s, 1H), 4.06 (dd, $J = 9.1, 7.2$ Hz, 1H), 3.75 (t, $J = 7.1$ Hz, 1H), 3.62 (t, $J = 8.7$ Hz, 1H), 1.84 (s, 3H), 1.00 (s, 9H), 0.05 (s, 3H), 0.02 (s, 3H); ^{13}C NMR (90 MHz, C_6D_6) δ 147.5, 140.4, 134.5, 132.9, 125.6, 122.4, 120.6, 120.3, 119.4, 112.2, 65.3, 48.5, 26.2, 18.6, 13.2, -5.1, -5.3; ES+ m/z (relative intensity) 314.2 (M + H, 100%); HRMS (ES+) calcd for $\text{C}_{19}\text{H}_{28}\text{NOSi}$: 314.1940, found 314.1944.

(39 h). (yellow oil): ^1H NMR (400 MHz, C_6D_6) δ 7.75 (d, $J = 7.7$ Hz, 1H), 7.47 (d, $J = 8.0$ Hz, 1H), 7.25 (t, $J = 7.2$ Hz, 1H), 7.19 (t, $J = 7.6$ Hz, 1H), 6.28 (s, 1H), 5.79 (s, 1H), 4.48 (t, $J = 6.0$ Hz, 1H), 3.78 (dd, $J = 10.0, 6.0$ Hz, 1H), 3.48 (dd, $J = 10.0, 6.0$ Hz, 1H), 1.87 (s, 3H), 0.89 (s, 9H), -0.05 (s, 3H), -0.12 (s, 3H); ^{13}C NMR (100 MHz, C_6D_6) δ 148.5, 135.4, 133.7, 129.9, 122.1, 121.5, 119.6, 110.5, 90.9, 65.2, 64.3, 26.0, 18.4, 12.4, -5.3 , -5.6 ; ES+ m/z (relative intensity) 314.2 (M + H, 100%), 627.4 (2 M + H, 25%); HRMS (ES+) calcd for $\text{C}_{19}\text{H}_{28}\text{NOSi}$: 314.1940, found 314.1951.

1-(tert-Butyl-dimethyl-silanyl)-3-methyl-1,4-dihydro-cyclopenta[b]indole (38i) and 3-(tert-Butyl-dimethyl-silanyl)-1-methyl-8H-3a-aza-cyclopent[a]indene (40i)

Method A: Following general procedure 4, with column chromatography performed at -78°C , 84 mg (0.27 mmol) of allene **25** produced 34 mg (44%) of **38i** as a yellow oil. Method B: Following general procedure 5, 75 mg (0.23 mmol) of allene **25** produced 22 mg (34%) of **38i** as a yellow oil. Method B: Following general procedure 6, 1005 mg (0.30 mmol) of allene **25** produced 21 mg (25%) of **38i** as a yellow oil and 7.4 mg (9%) of **40i** as a light yellow oil. **38i**: IR (neat): 3410 cm^{-1} ; ^1H NMR (360 MHz, CDCl_3) δ 7.95 (br s, 1H), 7.57 (m, 1H), 7.37 (m, 1H), 7.07 (m, 2H), 6.35 (app pent, $J = 1.8$ Hz, 1H), 3.43 (app pent, $J = 1.8$ Hz, 1H), 2.21 (t, $J = 1.8$ Hz, 3H), 0.87 (s, 9H), 0.24 (s, 3H), -0.36 (s, 3H); ^{13}C NMR (75 MHz, CDCl_3) δ 147.6, 140.3, 133.2, 127.9, 124.6, 123.2, 119.9, 119.3, 119.2, 111.7, 38.0, 27.3, 18.0, 12.8, -4.5 , -8.1 ; MS (ES+) m/z (relative intensity) 284.2 (M + H, 90%), 567.4 (2 M + H, 100%), 850.6 (3 M + H, 25%); HRMS (ES+) calcd for $\text{C}_{18}\text{H}_{26}\text{NSi}$: 284.1835, found 284.1837.

40iIR (neat): $2123, 1606\text{ cm}^{-1}$; ^1H NMR (360 MHz, C_6D_6) δ ppm: 7.68 (d, 1H, $J = 8.3$ Hz), 7.21 (s overlap w solvent, 1H), 7.11 (d, 1H, $J = 7.6$ Hz), 6.74 (s, 1H), 3.34 (s, 2H), 2.18 (s, 3H), 1.11 (s, 9H), 0.50 (s, 6H); ^{13}C NMR (90 MHz, C_6D_6) δ ppm: 143.5, 138.7, 135.6, 127.1, 126.1, 122.4, 122.4, 121.0, 111.9, 111.6, 27.6, 27.4, 18.2, 11.1, -3.1 ; MS (ES+) m/z (relative intensity) 284.2 (M + H, 100%); HRMS (ES+) calcd for $\text{C}_{18}\text{H}_{26}\text{NSi}$: 284.1835, found 284.1816.

1-[2-(tert-Butyl-dimethyl-silanyloxy)-ethyl]-2,3-dimethyl-1,4-dihydro-cyclopenta[b]indole (38m) and 3-[2-(tert-Butyl-dimethyl-silanyloxy)-ethyl]-1,2-dimethyl-8H-3a-aza-cyclopenta[a]indene (40m)

Method A: Following general procedure 4, with column chromatography performed at -78°C and irradiation performed at 350 nm, 75 mg (0.20 mmol) of allene **24** produced 29 mg (42%) of **38m** as a yellow oil. Method B: Following general procedure 5, with column chromatography on deactivated silica gel (2% $\text{H}_2\text{O}/\text{SiO}_2$), 100 mg (0.27 mmol) of allene **24** produced 6 mg (7%) of **38m** as a yellow oil and 37 mg (40%) of **40m** as a colorless oil. **38m**: IR (neat): 3401 cm^{-1} ; ^1H NMR (300 MHz, CDCl_3) δ 7.94 (br s, 1H), 7.53 (d, $J = 7.7$ Hz, 1H), 7.34 (dd, $J = 7.0, 0.9$ Hz, 1H), 7.08 (td, $J = 7.1, 0.9$ Hz, 1H), 7.01 (t, $J = 7.2$ Hz, 1H), 3.83 - 3.71 (m, 2H), 3.34 - 3.31 (m, 1H), 2.35 - 2.24 (m, 1H), 2.03 (d, $J = 1.0$ Hz, 3H), 2.01 (d, $J = 0.7$ Hz, 3H), 1.60 - 1.55 (m, 1H), 0.89 (s, 9H), 0.04 (s, 3H), 0.02 (s, 3H); ^{13}C NMR (90 MHz, CDCl_3) δ 148.4, 145.5, 139.3, 125.0, 124.1, 120.7, 119.9, 119.2, 117.9, 111.7, 61.4, 44.7, 33.9, 26.0, 18.3, 12.9, 10.4, -5.15 , -5.22 ; ES+ m/z (relative intensity) 342.2 (M + H, 100%); HRMS (AP+) calcd for $\text{C}_{21}\text{H}_{32}\text{NOSi}$: 342.2253, found 342.2239.

40m: IR (neat): $2857, 1607, 1098\text{ cm}^{-1}$; ^1H NMR (300 MHz, C_6D_6) δ ppm: 7.32 (d, 1H, $J = 3.9$ Hz), 7.05 (t, 2H, $J = 7.0$ Hz), 6.86 (dt, 1H, $J = 3.7, 0.9$ Hz), 3.81 (t, 2H, $J = 7.5$ Hz), 3.32 (bs, 2H), 3.13 (t, 2H, $J = 7.4$ Hz), 2.07 (s, 3H), 2.02 (s, 3H), 0.93 (s, 9H), -0.02 (s, 6H); ^{13}C NMR (C_6D_6) δ ppm: 145.0, 136.1, 130.9, 126.0, 121.8, 120.8, 119.6, 110.5, 110.4, 63.3, 29.4, 27.5, 26.1, 18.1, 9.9, 9.7, -5.4 ; ES+ m/z (relative intensity) 342.2 (M + H, 100%); HRMS (ES+) calcd for $\text{C}_{21}\text{H}_{32}\text{NOSi}$: 342.2253, found 342.2253.

6,9,9-Trimethyl-5,7,8,9,10,10a-hexahydro-indeno[2,1-b]indol-10-ol (42a) and 3,3,1,1-Trimethyl-2,3-dihydro-1H-indolo[1,2-a]indole (44)

Method A: Following general procedure 4, 109 mg (0.369 mmol) of allene **29** produced 59 mg (60%) of **42a** as a brown solid. Method B: Following general procedure 5, 350 mg (1.18 mmol) of allene **29** produced 107 mg (34%) of **42a** as a brown solid and 72 mg (25%) of **44^{1b}** as a brown solid. Method C: Following general procedure 6, 78 mg (0.26 mmol) of allene **29** produced 15 mg (21%) of **42a** as a brown solid and 16 mg (24%) of **44** as a brown solid.

42a: mp. 76 °C (dec.); IR (neat): 3400, 3301 cm^{-1} ; ^1H NMR (400 MHz, C_6D_6) δ 7.94 (d, $J = 7.7$ Hz, 1H), 7.29 - 7.20 (m, 3H), 6.99 (br s, 1H), 3.26 (d, $J = 10.7$ Hz, 1H), 2.56 (dd, $J = 10.7$, 4.8 Hz, 1H), 2.34 (dd, $J = 14.2$, 3.0 Hz, 1H), 2.16 (td, $J = 14.2$, 3.2 Hz, 1H), 1.80 - 1.75 (m, 1H), 1.77 (s, 3H), 1.44 (dd, $J = 13.1$, 3.2 Hz, 1H), 1.08 (s, 3H), 1.08 - 0.99 (m, 1H), 0.91 (s, 3H); ^{13}C NMR (90 MHz, CDCl_3) δ 148.9, 145.5, 139.3, 125.0, 122.5, 120.7, 120.1, 119.5, 118.3, 111.8, 82.6, 49.1, 40.7, 36.2, 28.0, 22.7, 17.5, 10.2; APCI+ m/z (relative intensity) 268.2 (M + H, 100%); HRMS (ES+) calcd for $\text{C}_{18}\text{H}_{22}\text{NO}$: 268.1701, found 268.1714.

4-(tert-Butyl-dimethyl-silanyloxy)-3,3-dimethyl-11-trimethyl-silanylmethyl-2,3,4,4a-tetrahydro-1H-indolo[1,2-a]indole (43e) and 2-{1-[3-(tert-Butyl-dimethyl-silanyloxy)-4,4-dimethyl-cyclohex-1-enyl]-vinyl}-1H-indole (45e)

Method A: Following General Procedure 5, 135 mg (0.28 mmol) of **28e** produced 45 mg (35%) of **43e** as a white solid and 44 mg (41%) of **45e** as a brown oil. Method B: Following General Procedure 6, 60 mg (0.12 mmol) of **28e** produced 28 mg (50%) of **43e** as a white solid and 5 mg (11%) of **45e** as a brown oil. Crystals of **43e** suitable for X-ray crystallographic analysis were obtained by slow evaporation of an Et_2O /hexanes solution of **43e** over a period of 24 h at rt. mp. 105 - 106 °C. **43e**: IR (neat): 1456 cm^{-1} ; ^1H NMR (300 MHz, CDCl_3) δ 7.49 (m, 2H), 7.00 (m, 2H), 6.08 (s, 1H), 4.55 (d, $J = 9.3$ Hz, 1H), 3.10 (d, $J = 9.4$ Hz, 1H), 2.48 (dd, $J = 14.2$, 5.5 Hz, 1H), 2.31 (td, $J = 12.9$, 5.1 Hz, 1H), 1.87 (s, 2H), 1.63 (dd, $J = 13.4$, 4.0 Hz, 1H), 1.33 (m, 1H), 1.15 (s, 3H), 1.00 (s, 12H), 0.06 (s, 9H), -0.06 (s, 3H), -0.84 (s, 3H); ^{13}C NMR (75 MHz, CDCl_3) δ 151.3, 139.6, 137.0, 132.3, 125.0, 120.7, 119.7, 118.8, 112.3, 90.8, 84.1, 65.6, 39.1, 37.8, 29.9, 26.6, 22.7, 18.5, 18.4, 15.5, -0.9, -2.3, -3.7; ES+ m/z (relative intensity) 454.3 (M + H, 100%); HRMS (ES+) calcd for $\text{C}_{27}\text{H}_{44}\text{NOSi}_2$: 454.2961, found 454.2949.

45e: IR (neat): 3412 cm^{-1} ; ^1H NMR (300 MHz, CDCl_3) δ 8.05 (br s, 1H), 7.56 (dd, $J = 8.2$, 1.1 Hz, 1H), 7.31 (dd, $J = 8.0$, 0.8 Hz, 1H), 7.16 (td, $J = 7.0$, 1.2 Hz, 1H), 7.08 (td, $J = 7.1$, 1.2 Hz, 1H), 6.52 (dd, $J = 2.1$, 0.9 Hz, 1H), 5.79 (pent, $J = 1.6$ Hz, 1H), 5.34 (s, 1H), 5.22 (s, 1H), 3.88 (dd, $J = 4.9$, 2.0 Hz, 1H), 2.25 (m, 2H), 1.65 (m, 1H), 1.45 (m, 1H), 0.96 (s, 3H), 0.92 (s, 3H), 0.90 (s, 9H), 0.05 (s, 3H), 0.00 (s, 3H); ^{13}C NMR (75 MHz, CDCl_3) δ 142.3, 137.4, 136.4, 136.0, 131.2, 128.6, 122.2, 120.6, 119.9, 111.9, 110.6, 102.4, 74.7, 33.8, 33.3, 26.8, 25.9, 25.4, 21.4, 18.2, -4.1, -4.9; ES+ m/z (relative intensity) 382.2 (M + H, 100%); HRMS (ES+) calcd for $\text{C}_{24}\text{H}_{36}\text{NOSi}$: 382.2566, found 382.2555.

6,9,9-Trimethyl-10-(2-trimethylsilanyl-ethoxymethoxy)-5,7,8,9,10,10a-hexahydro-indeno[2,1-b]indole (42f) and 3,3,1,1-Trimethyl-2,3-dihydro-1H-indolo[1,2-a]indole (44)

Method A: Following general procedure 4, 84 mg (0.20 mmol) of allene **28c** produced 47 mg (60%) of **42f** as a yellow solid. Method B: Following general procedure 5, 67 mg (0.16 mmol) of allene **28c** produced 22 mg (35%) of **42f** as a yellow solid and 20 mg (51%) of **44^{1b}** as a yellow solid. Method C: Following general procedure 6, 57 mg (0.13 mmol) of allene **28c** produced 20 mg (38%) of **42f** as a yellow solid and 17 mg (51%) of **44** as a yellow solid. **42f**: mp. 139 - 140 °C; IR (neat): 3405 cm^{-1} ; ^1H NMR (400 MHz, CDCl_3) δ 7.99 (br s, 1H), 7.55 (d, $J = 7.8$ Hz, 1H), 7.32 (d, $J = 7.8$ Hz, 1H), 7.09 (t, $J = 7.1$ Hz, 1H), 7.03 (t, $J = 7.6$ Hz, 1H), 4.91 (d, $J = 6.8$ Hz, 1H), 4.61 (d, $J = 6.8$ Hz, 1H), 3.87 (m, 1H), 3.52 (m, 1H), 3.38 (d, $J = 10.5$ Hz, 1H), 2.73 (d, $J = 10.7$ Hz, 1H), 2.54 (m, 1H), 2.36 (m, 1H), 2.01 (s, 3H), 1.66 (m, 1H),

1.30 (m, 1H), 1.21 (s, 3H), 1.08 (s, 3H), 0.91 (m, 1H), 0.00 (s, 9H); ^{13}C NMR (100 MHz, CDCl_3) δ 149.2, 145.9, 139.3, 125.3, 122.3, 120.1, 120.0, 119.4, 118.6, 111.7, 96.8, 89.7, 65.8, 48.7, 41.3, 36.5, 28.7, 22.7, 18.7, 18.0, 10.2, -1.5; ES+ m/z (relative intensity) 398.7 (M + H, 100%), 420.7 (M + Na, 40%); HRMS (ES+) calcd for $\text{C}_{24}\text{H}_{36}\text{NO}_2\text{Si}$: 398.2515, found 398.2521.

10-(tert-Butyl-dimethyl-silyloxy)-6-(tert-butyl-dimethyl-silyloxymethyl)-9,9-dimethyl-5,7,8,9,10,10a-hexahydro-indeno[2,1-b]indole (42 g)

Following general procedure 4, allene **37** (99 mg, 0.18 mmol) produced 54 mg (59%) of **42g** as a tacky yellow solid: IR (neat): 3483 cm^{-1} ; ^1H NMR (300 MHz, CDCl_3) δ 8.20 (br s, 1H), 7.65 (m, 1H), 7.34 (m, 1H), 7.01 – 7.10 (m, 2H), 4.73 (d, $J = 13.2$ Hz, 1H), 4.64 (d, $J = 13.2$ Hz, 1H), 3.41 (d, $J = 10.3$ Hz, 1H), 3.07 (d, $J = 10.3$ Hz, 1H), 2.52 (ddd, $J = 14.2, 5.6, 1.8$ Hz, 1H), 2.36 – 2.47 (m, 1H), 1.67 (ddd, $J = 13.1, 5.3, 1.8$ Hz, 1H), 1.36 (dd, $J = 13.1, 5.6$ Hz, 1H), 1.19 (s, 3H), 1.07 (s, 9H), 1.02 (s, 3H), 0.95 (s, 9H), 0.13 (s, 3H), 0.11 (s, 3H), -0.02 (s, 3H), -0.45 (s, 3H); ^{13}C NMR (75 MHz, CDCl_3) δ 148.5, 146.2, 139.2, 127.2, 126.0, 121.8, 120.4, 119.5, 118.7, 111.4, 82.9, 58.6, 50.0, 40.3, 37.7, 29.9, 26.6, 26.0, 23.4, 18.6, 18.4, 18.3, -1.9, -3.0, -5.1, -5.2; ES+ m/z (relative intensity) 512.2 (M + H, 100%); HRMS (ES+) calcd for $\text{C}_{30}\text{H}_{50}\text{NO}_2\text{Si}_2$: 512.3380, found 512.3379.

6,9,9-Trimethyl-8,9-dihydro-7H-indeno[2,1-b]indole-5-carboxylic Acid tert-Butyl Ester (46)

To a 0 °C stirring solution of alcohol **42a** (198 mg, 0.741 mmol) in 7.5 mL of CH_2Cl_2 was added DMAP (904 mg, 7.41 mmol) and Boc_2O (403 mg, 1.85 mmol) sequentially and then the reaction was warmed to rt and stirred for 1 h. The solvent was then removed under reduced pressure and the residue was dissolved in Et_2O (15 mL) and washed with H_2O (3×15 mL), and brine (3×15 mL), dried over MgSO_4 , and concentrated under reduced pressure. The residue was purified by flash chromatography (5% Et_2O /hexanes) to provide 150 mg (58%) of **46** as an orange oil: IR (neat): 1736 cm^{-1} ; ^1H NMR (400 MHz, CDCl_3) δ 8.01 (dd, $J = 8.3, 0.8$ Hz, 1H), 7.51 (d, $J = 7.6$ Hz, 1H), 7.17 (td, $J = 7.5, 1.0$ Hz, 1H), 7.10 (ddd, $J = 8.5, 7.3, 1.4$ Hz, 1H), 6.58 (s, 1H), 2.64 (td, $J = 6.0, 1.3$ Hz, 2H), 2.23 (s, 3H), 1.75 (t, $J = 6.7$ Hz, 2H), 1.69 (s, 9H), 1.20 (s, 6H); ^{13}C NMR (100 MHz, CDCl_3) δ 150.2, 148.7, 141.9, 139.7, 133.6, 132.4, 125.5, 124.8, 123.0, 121.7, 117.6, 116.8, 116.3, 83.9, 38.6, 33.7, 28.4, 28.3, 20.5, 14.0; ES+ m/z (relative intensity) 350.2 (M + H, 100%); HRMS (ES+) calcd for $\text{C}_{23}\text{H}_{28}\text{NO}_2$: 350.2120, found 350.2124.

6,6,9,9-Tetramethyl-7,8,9,10-tetrahydro-6H-indeno[2,1-b]indole-5-carboxylic Acid tert-Butyl Ester (47)

To a -40 °C stirring solution of fulvene **46** (27 mg, 0.077 mmol) in 4 mL of THF was added LiAlH_4 (1.0 M in THF, 120 μL , 0.12 mmol) and the reaction solution was allowed to warm to rt. CH_3I (15 μL , 0.24 mmol) was then added and stirring was continued for 30 min, then ice-cold saturated NH_4Cl (4 mL) was added slowly and the mixture was diluted with Et_2O (15 mL). The organic layer was washed with H_2O (3×15 mL) and brine (3×15 mL), dried over MgSO_4 and concentrated under reduced pressure. The residue was purified by flash chromatography (5% Et_2O /hexanes) to provide 24 mg (85%) of **47** as a yellow oil: IR (neat): 1729 cm^{-1} ; ^1H NMR (360 MHz, CDCl_3) δ 8.14 (m, 1H), 7.56 (m, 1H), 7.20 - 7.17 (m, 2H), 2.41 (t, $J = 2.3$ Hz, 2H), 2.15 - 2.12 (m, 2H), 1.71 (s, 9H), 1.54 (t, $J = 6.2$ Hz, 2H), 1.39 (s, 6H), 1.00 (s, 6H); ^{13}C NMR (90 MHz, CDCl_3) δ 151.8, 150.1, 145.0, 139.5, 127.4, 126.4, 124.4, 122.7, 122.5, 118.6, 116.4, 83.7, 48.5, 37.5, 35.9, 29.7, 28.4, 28.2, 20.6, 19.0; ES+ m/z (relative intensity) 366.3 (M + H, 100%); HRMS (ES+) calcd for $\text{C}_{24}\text{H}_{32}\text{NO}_2$: 366.2433, found 366.2446.

(E)-3-Iodo-2-phenyl-prop-2-en-1-ol (58b)

A solution of (Z)-3-Iodo-2-phenyl-prop-2-en-1-ol (**58a**)²⁵ (1.12 g, 4.31 mmol) in 160 mL of CH₃CN was irradiated at 254 nm for 2 h and then concentrated under reduced pressure. ¹H NMR analysis of the reaction mixture indicated that it contained a 5:1 mixture of the *E* and *Z* isomers, respectively. The residue was purified by flash chromatography (hexanes → 4% EtOAc/hexanes → 8% EtOAc/hexanes) to provide 157 mg (14%) of the starting material **58a** and 400 mg (36%) of **58b** as a white solid: mp. 58–59 °C; IR (neat): 3321 cm⁻¹; ¹H NMR (360 MHz, CDCl₃) δ 7.28–7.21 (m, 3H), 7.11–7.09 (m, 2H), 6.49 (s, 1H), 4.19 (s, 2H), 2.27 (br s, 1H); ¹³C NMR (90 MHz, CDCl₃) δ 151.7, 139.5, 128.5, 128.1, 128.0, 78.3, 67.3; EI+ *m/z* (relative intensity) 260.3 (M⁺, 100%); HRMS (EI+) calcd for C₉H₉OI 259.9698, found 259.9704.

(E)-tert-Butyldimethyl(2-phenylpent-2-en-4-ynoxy)silane (59)

To a stirring solution of alcohol **58b** (395 mg, 1.52 mmol) in 10 mL of Et₃N were added trimethylsilylacetylene (433 μL, 3.04 mmol), PdCl₂(PPh₃)₂ (21 mg, 0.30 mmol), and CuI (3 mg, 0.02 mmol), and the reaction mixture was stirred for 24 h at rt and then diluted with Et₂O. The mixture was washed with saturated NH₄Cl solution (3 × 50 mL), H₂O (3 × 50 mL), and brine (3 × 50 mL), dried over MgSO₄, and concentrated under reduced pressure. The crude residue was purified by flash chromatography (hexanes → 5% Et₂O/hexanes → 25% Et₂O/hexanes) to provide 215 mg (54%) of the corresponding TMS-alkyne. TBAF (1.0 M in THF, 1 mL, 1 mmol) was added slowly to a solution of the above TMS-alkyne (215 mg, 0.933 mmol) in 10 mL of THF and stirred for 20 min. Saturated NaHCO₃ (10 mL) was added, and the organic layer was washed with H₂O (3 × 30 mL) and brine (3 × 30 mL), dried over MgSO₄, and concentrated under reduced pressure. The residue was dissolved in CH₂Cl₂ (6 mL). Imidazole (95 mg, 1.4 mmol) and TBSCl (211 mg, 1.40 mmol) were added sequentially, and the reaction solution was stirred for 20 min, then H₂O (10 mL) was added slowly, and the reaction mixture was diluted with Et₂O (50 mL). The organic layer was washed with H₂O (3 × 50 mL) and brine (3 × 50 mL), dried over MgSO₄, and concentrated under reduced pressure. The residue was purified by flash chromatography (hexanes → 5% Et₂O/hexanes) to provide 228 mg (90%) of **59** as a yellow oil: IR (neat) 3294 cm⁻¹; ¹H NMR (400 MHz, CDCl₃) δ 7.49–7.46 (m, 2H), 7.39–7.29 (m, 3H), 5.94 (app q, *J* = 2.3 Hz, 1H), 4.45 (dd, *J* = 2.0, 0.7 Hz, 2H), 2.90 (d, *J* = 2.5 Hz, 1H), 0.94 (s, 9H), 0.10 (s, 6H); ¹³C NMR (90 MHz, CDCl₃) δ 153.1, 137.0, 128.2, 128.1, 127.7, 103.5, 81.6, 80.6, 65.4, 25.8, 18.3, -5.4; ES+ *m/z* (relative intensity) 273.2 (M + H, 100%); HRMS (ES+) calcd for C₁₇H₂₅OSi: 273.1675, found 273.1664.

Acetic Acid 1-(2-Azidophenyl)-6-(tert-butyldimethylsilyloxy)-5-phenylhex-4-en-2-ynyl Ester (60)

To a -30 °C stirring solution of alkyne **59** (278 mg, 0.837 mmol) in 8 mL of THF was added slowly *n*-BuLi (2.5 M in hexanes, 340 μL, 0.84 mmol). Stirring was continued for 1 h, and then a solution of 2-azidoben-zaldehyde (123 mg, 0.837 mmol) in 8 mL of THF was added. Stirring was continued for 20 min (as monitored by TLC for starting material consumption), and then Ac₂O (119 μL, 1.26 mmol) was added, and the reaction solution was allowed to warm to rt. Ice-cold saturated NH₄Cl (10 mL) was added dropwise, and the mixture was diluted with Et₂O (25 mL). The organic layer was washed with H₂O (3 × 25 mL) and brine (3 × 25 mL), dried over MgSO₄, and concentrated under reduced pressure. The residue was purified by flash chromatography (5% Et₂O/hexanes → 15% Et₂O/hexanes) to provide 320 mg (83%) of **60** as a yellow oil: IR (neat) 2126, 1746 cm⁻¹; ¹H NMR (360 MHz, CDCl₃) δ 7.35–7.32 (m, 2H), 7.30 (dd, *J* = 7.7, 1.1 Hz, 1H), 7.24 (td, *J* = 7.9, 1.4 Hz, 1H), 7.21–7.18 (m, 3H), 7.00–6.92 (m, 2H), 6.59 (d, *J* = 1.5 Hz, 1H), 5.91 (app q, *J* = 2.0 Hz, 1H), 4.37 (d, *J* = 1.7 Hz, 2H), 1.94 (s, 3H), 0.84 (s, 9H), 0.00 (s, 6H); ¹³C NMR (90 MHz, CDCl₃) δ 169.3, 153.1, 137.6, 137.0, 130.0, 129.4, 128.02, 127.95, 127.8, 127.7, 124.7, 118.0, 103.6, 88.0, 85.3, 65.3, 61.4, 25.8, 20.8,

18.2, -5.5; ES+ m/z (relative intensity) 484.1 (M + Na, 80), 507.2 (M + 2Na, 70); HRMS (ES+) calcd for C₂₆H₃₁N₃O₃SiNa 484.2032, found 484.2033.

[4-(2-Azidobenzyl)-3-methylnaphthalen-1-ylmethoxy]-*tert*-butyldimethylsilane (61)

Following general procedure 3, 320 mg (0.693 mmol) of **60** produced 120 mg (41%) of **61** as a tacky yellow solid: IR (neat) 2120 cm⁻¹; ¹H NMR (360 MHz, CDCl₃) δ 7.73 (dd, $J = 7.5$, 1.7 Hz, 1H), 7.54 (dd, $J = 7.6$, 1.8 Hz, 1H), 7.17–7.13 (m, 2H), 6.97–6.90 (m, 3H), 6.56 (td, $J = 7.1$, 2.0 Hz, 1H), 6.23 (d, $J = 7.8$ Hz, 1H), 4.96 (s, 2H), 4.08 (s, 2H), 2.17 (s, 3H), 0.74 (s, 9H), -0.08 (s, 6H); ¹³C NMR (90 MHz, CDCl₃) δ 137.7, 135.2, 134.2, 132.9, 131.53, 131.48, 129.9, 129.0, 127.28, 127.25, 127.1, 125.9, 124.8, 124.6, 123.7, 117.6, 63.4, 28.9, 26.0, 20.4, 18.5, -5.2; ES+ m/z (relative intensity) 418.3 (M + H, 100), 435.3 (M + NH₄, 70), 440.3 (M + Na, 70); HRMS (ES+) calcd for C₂₅H₃₂N₃O₃Si 418.2315, found 418.2322.

Supplementary Material

Refer to Web version on PubMed Central for supplementary material.

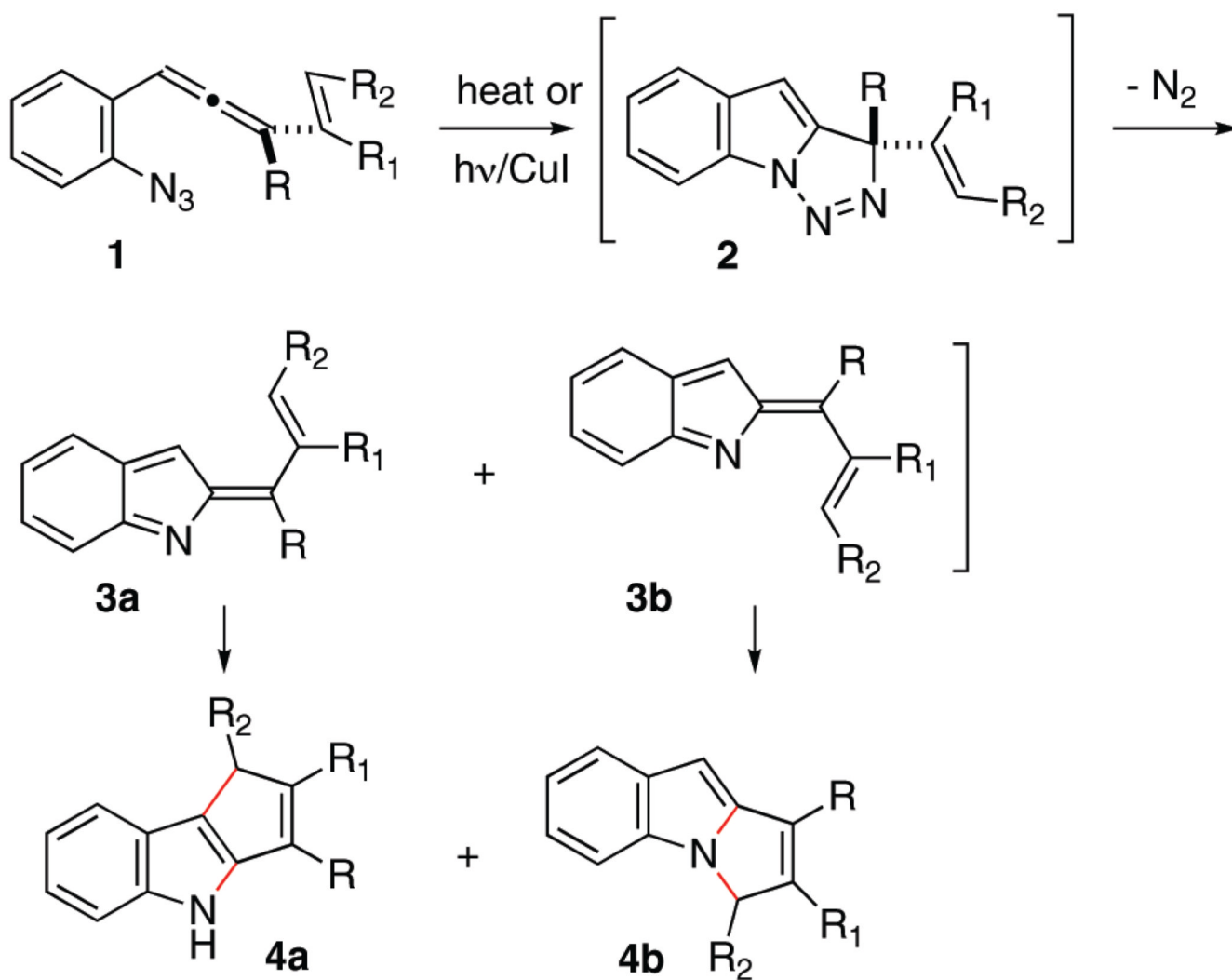
References

- (a) Feldman KS, Iyer MR, Hester DK II. *Org. Lett* 2006;8:3113–3116. [PubMed: 16805565] (b) Feldman KS, Hester DK II, López CS, Faza ON. *Org. Lett* 2008;10:1665–1668. [PubMed: 18345683]
- López CS, Faza ON, Feldman KS, Iyer MR, Hester DK II. *J. Am. Chem. Soc* 2007;129:7638–7646. [PubMed: 17530848]
- (a) Park A, Moore RE, Patterson GML. *Tetrahedron Lett* 1992;33:3257–3260. (b) Stratmann K, Moore RE, Bonjouklian R, Deeter JB, Patterson GML, Shaffer S, Smith CD, Smitka TA. *J. Am. Chem. Soc* 1994;116:9935–9942.
- Ondeyka JG, Helms GL, Hensens OD, Goetz MA, Zink DL, Tsipouras A, Shoop WL, Slayton L, Dombrowski AW, Polishook JD, Ostlind DA, Tsou NN, Ball RG, Singh SB. *J. Am. Chem. Soc* 1997;119:8809–8816.
- Irlinger B, Bartsch A, Krämer H-J, Mayser P, Steglich W. *Helv. Chim. Acta* 2005;88:1472–1485.
- Gross G, Wentrup C. *J. Chem. Soc. Chem. Commun* 1982;360
- (a) Büchi G, Manning RE. *J. Am. Chem. Soc* 1966;88:2532. (b) Kutney JP, Beck J, Bylsma F, Cretney WJ. *J. Am. Chem. Soc* 1968;90:4504. [PubMed: 5666353] (c) Potier P, Langlois Y, Gueritte F. *J. Chem. Soc., Chem. Commun* 1975:670–671. (d) Kutney JP, Ratcliffe AH, Treasurywala AM, Wunderly S. *Heterocycles* 1975;3:639–649. (e) Schill G, Priester CU, Windhovel UF, Fritz H. *Tetrahedron* 1987;43:3765–3786. (f) Magnus P, Stamford A, Ladlow M. *J. Am. Chem. Soc* 1990;112:8210–8212. (g) Yokoshima S, Ueda T, Kobayashi S, Sato A, Kuboyama T, Tokuyama H, Fukuyama T. *J. Am. Chem. Soc* 2002;124:2137–2139. [PubMed: 11878966] (h) Ishikawa H, Colby DA, Boger DL. *J. Am. Chem. Soc* 2008;130:420–421. [PubMed: 18081297]
- Jansen A, Krause N. *Synthesis* 2002:1987–1992.
- Piers E, Grierson JR, Lau CK, Nagakura I. *Can. J. Chem* 1982;60:210–223.
- Feldman KS, Iyer MR. *J. Am. Chem. Soc* 2005;127:4590–4591. [PubMed: 15796521]
- Kashulin IA, Nifant'ev IE. *J. Org. Chem* 2004;69:5476–5479. [PubMed: 15287801]
- Cambridge Crystallographic Data Centre deposition numbers: **39n**, 649706; **40a**, 619622; **42b**, 650218, **42d**, 652945; **43e**, 650217; **54**, 651276. The data can be obtained free of charge from the Cambridge Data Centre via http://www.ccdc.cam.ac.uk/data_request/cif.
- (a) Hirsch JA. *Top. Stereochem* 1967;1:199–222. (b) Eliel EL, Satici H. *J. Org. Chem* 1994;59:688–689. (c) Crich D, Jayalath P, Hutton TK. *J. Org. Chem* 2006;71:3064–3070. [PubMed: 16599600]
- Mukai C, Kobayashi M, Kubota S, Takahashi Y, Kitagaki S. *J. Org. Chem* 2004;69:2128–2136. [PubMed: 15058962]
- (a) Hohenberg P, Kohn W. *Phys. Rev* 1964;136:B864–B871. (b) Kohn W, Sham L. *Phys. Rev. A* 1965;140:A1133–A1138. (c) Stephens PJ, Devlin FJ, Chabalowski CF, Frisch MJ. *J. Phys. Chem*

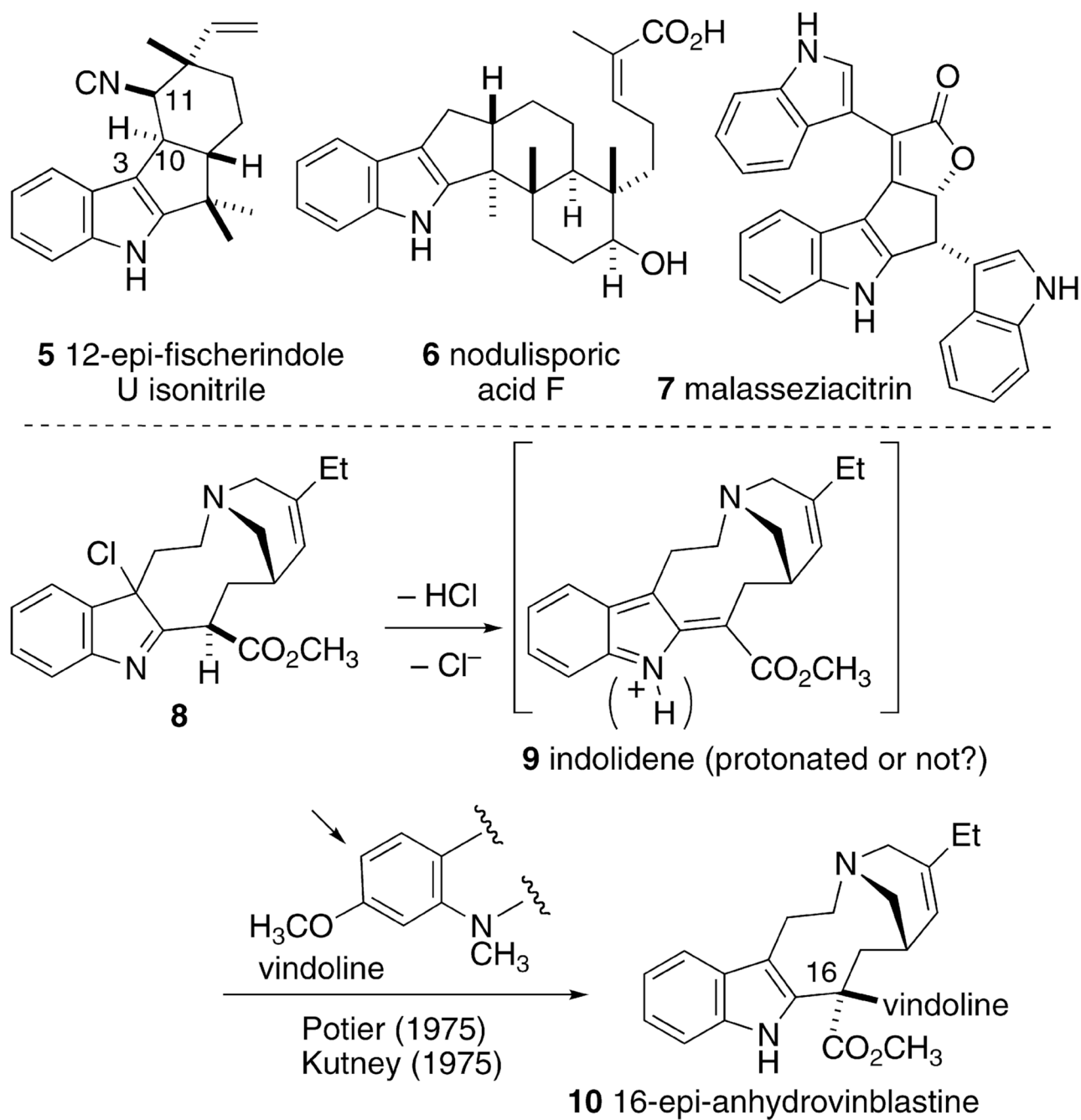
- 1994;98:11623–11637. (d) Becke AD. *J. Chem. Phys* 1993;98:5648–5652. (e) Lee C, Yang W, Parr RG. *Phys. Rev. B* 1988;37:785–789.
16. Woodward, RB.; Hoffmann, R. *The Conservation of Orbital Symmetry*. Weinheim: VCH; 1970.
17. (a) Herges R, Geuenich D. *J. Phys. Chem. A* 2001;105:3214–3220. (b) Geuenich D, Hess K, Koehler F, Herges R. *Chem. Rev* 2005;105:3758–3772. [PubMed: 16218566]
18. Schleyer, PvR; Maerker, C.; Dransfeld, A.; Jiao, H.; Hommes, NJRvE. *J. Am. Chem. Soc* 1996;118:6317–6318.
19. (a) Li Z, Quan RW, Jacobsen EN. *J. Am. Chem. Soc* 1995;117:5889–5890. (b) Brandt P, Södergren MJ, Andersson PG, Norrby P-O. *J. Am. Chem. Soc* 2000;122:8013–8020. (c) Bertz SH, Cope S, Murphy M, Ogle CA, Taylor BJ. *J. Am. Chem. Soc* 2007;129:7208–7209. [PubMed: 17506552]
20. (a) Hohenberg P, Kohn W. *Phys. Rev* 1964;136:B864–B871. (b) Kohn W, Sham L. *Phys. Rev. A* 1965;140:A1133–A1138. (c) Stephens PJ, Devlin FJ, Chabalowski CF, Frisch MJ. *J. Phys. Chem* 1994;98:11623–11637. (d) Becke AD. *J. Chem. Phys* 1993;98:5648–5652. (e) Lee C, Yang W, Parr RG. *Phys. Rev. B* 1988;37:785–789.
21. Frisch, MJ., et al. *Gaussian03, revision C.02*. Wallingford, CT: Gaussian, Inc; 2004.
22. Bauernschmitt R, Ahlrichs R. *J. Chem. Phys* 1996;22:9047–9052.
23. (a) Hess BA Jr, Eckart U, Fabian J. *J. Am. Chem. Soc* 1998;120:12310–12315. (b) Hess BA Jr, Smentek L, Brash AR, Cha JK. *J. Am. Chem. Soc* 1999;121:5603–5604. (c) López CS, Faza ON, York DM, de Lera A. *J. Org. Chem* 2004;69:3635–3644. [PubMed: 15152991] (d) Li J, Worthington SE, Cramer CJ. *J. Chem. Soc., Perkin Trans. 2* 1998:1045–1052.
24. Huang Z, Negishi E-i. *Org. Lett* 2006;8:3675–3678. [PubMed: 16898789]
25. Duboudin JG, Jousseume B, Bonakdar A. *J. Organomet. Chem* 1979;168:227–232.

Acknowledgments

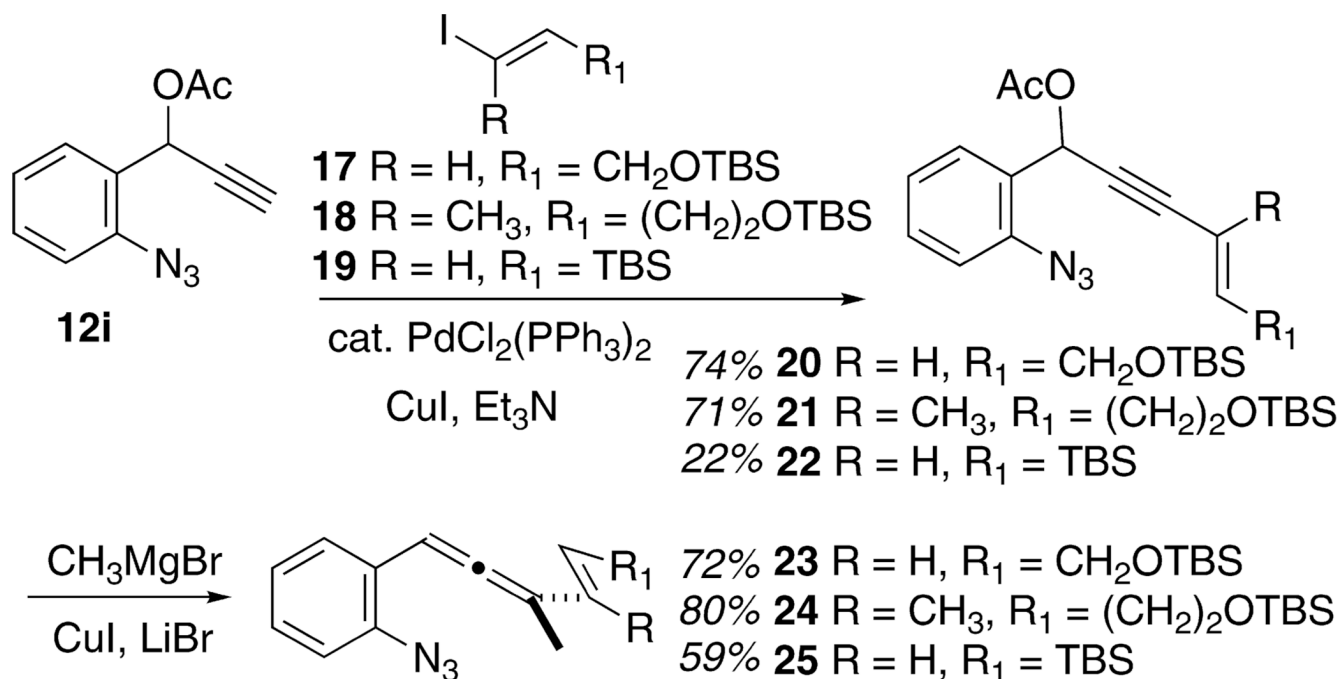
Support from the National Institutes of Health, General Medical Sciences division (GM72572), and the National Science Foundation for the X-ray Crystallography Facility (CHE 0131112), is gratefully acknowledged. C.S.L. is grateful to CESGA for supercomputer time.



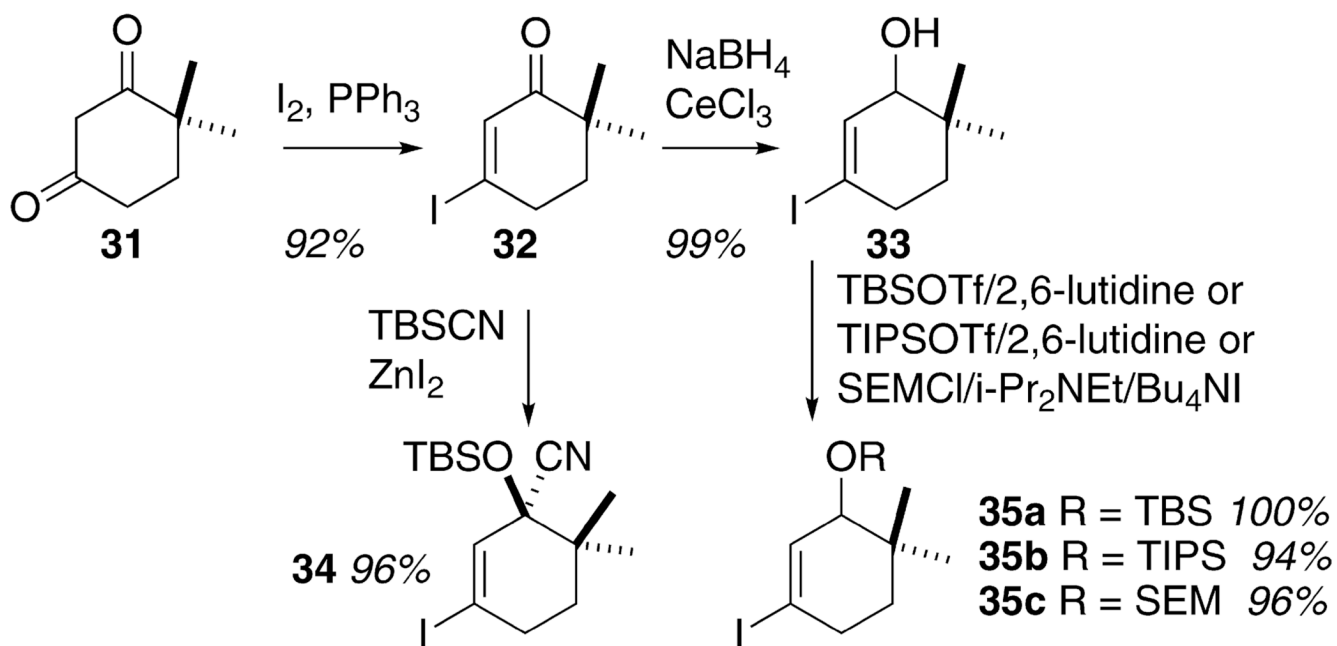
SCHEME 1.
 Cyclization Cascade of 1-(2-Azidophenyl)-3-vinylallenes
^aThe new bonds are indicated in red.



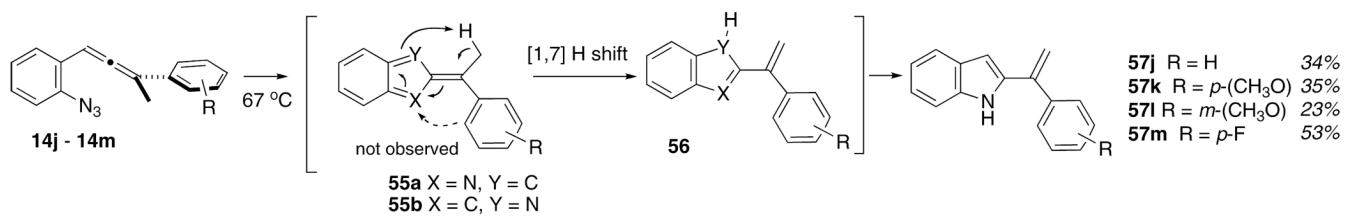
SCHEME 2.
 Representative 2,3-Cyclopentannellated Indole Natural Products and the Historical Precedent for Invoking Indolidenes in Indole-Containing Natural Product Synthesis



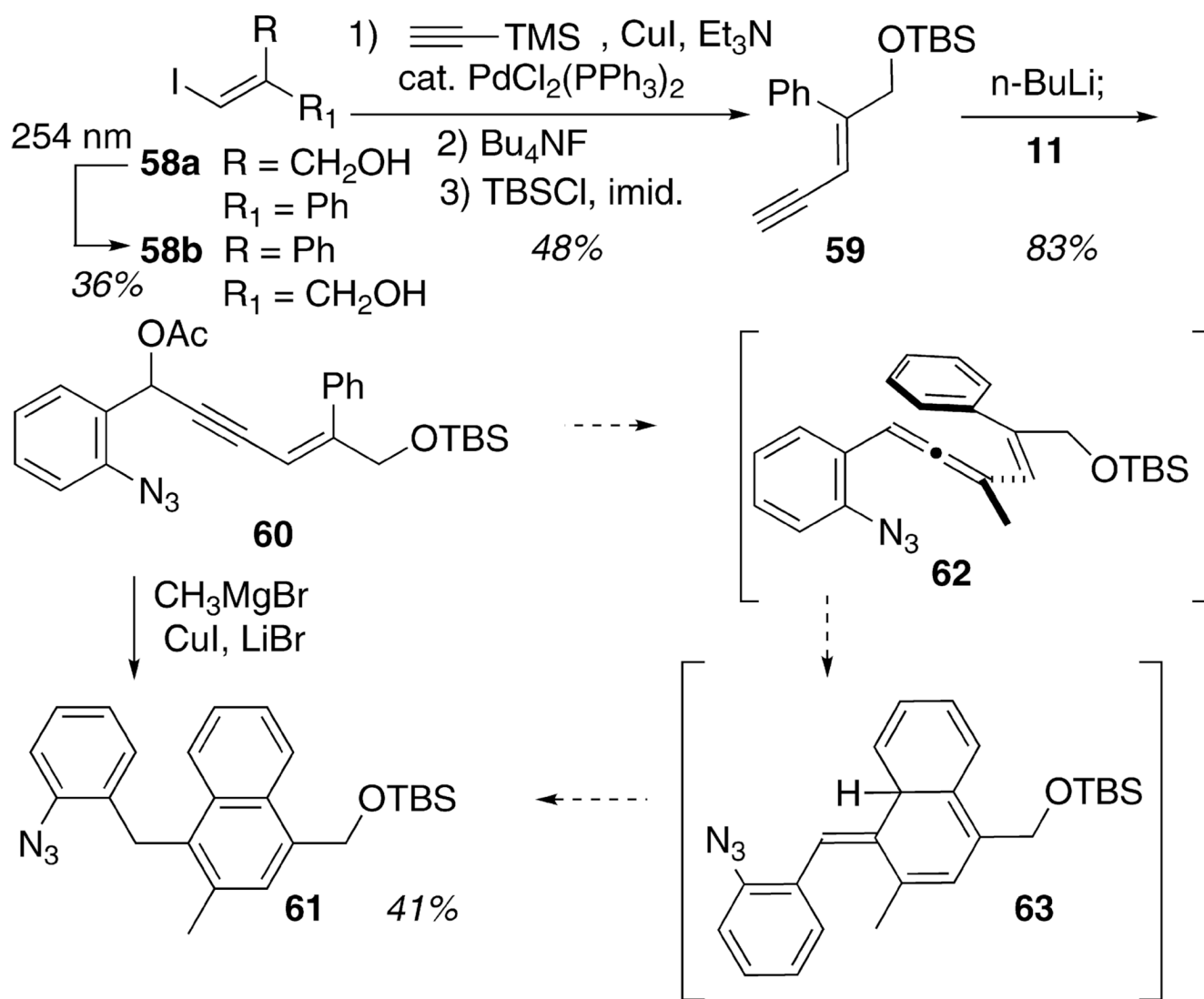
SCHEME 3.
 Synthesis of Additional (*o*-Azidophenyl)allenes



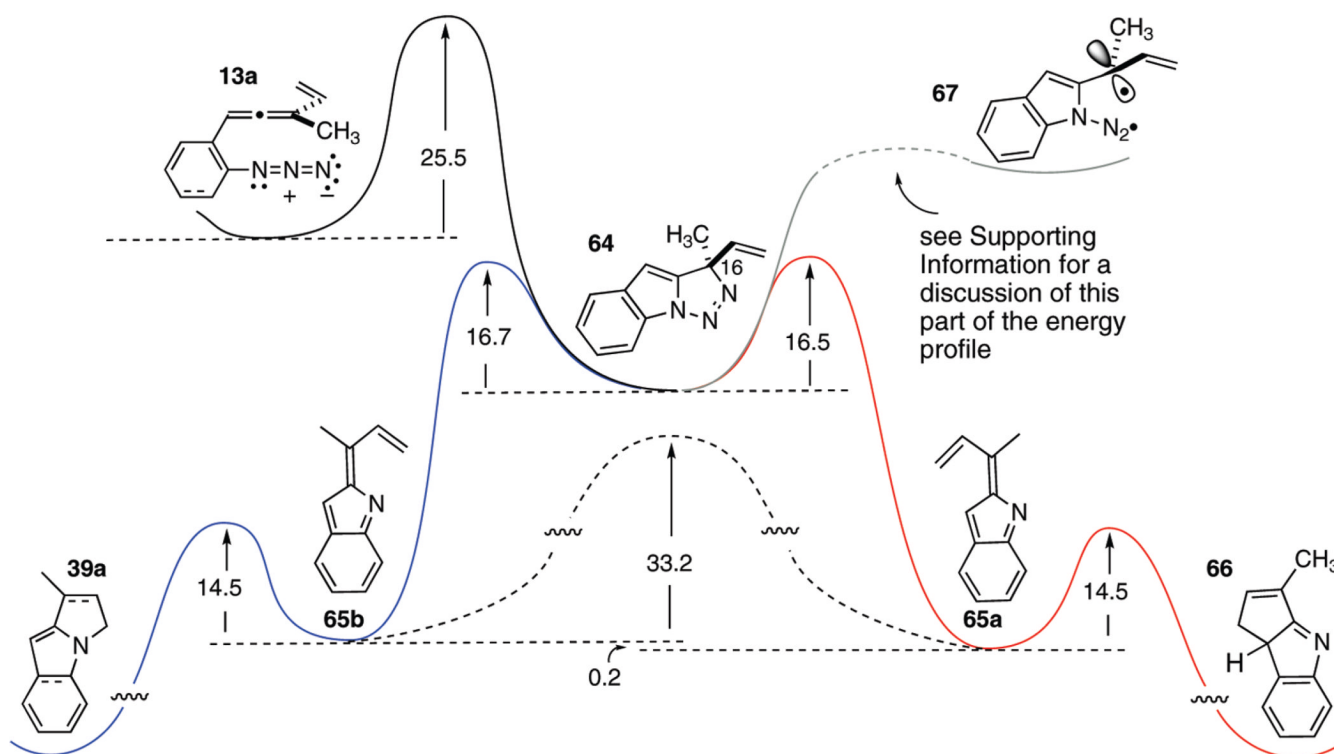
SCHEME 4.
Preparation of Functionalized Cyclohexenyl Iodides



SCHEME 5.
 Cascade Cyclization Attempts with Aryl-Substituted 1-(2-Azidophenyl)allene Substrates 14j–m

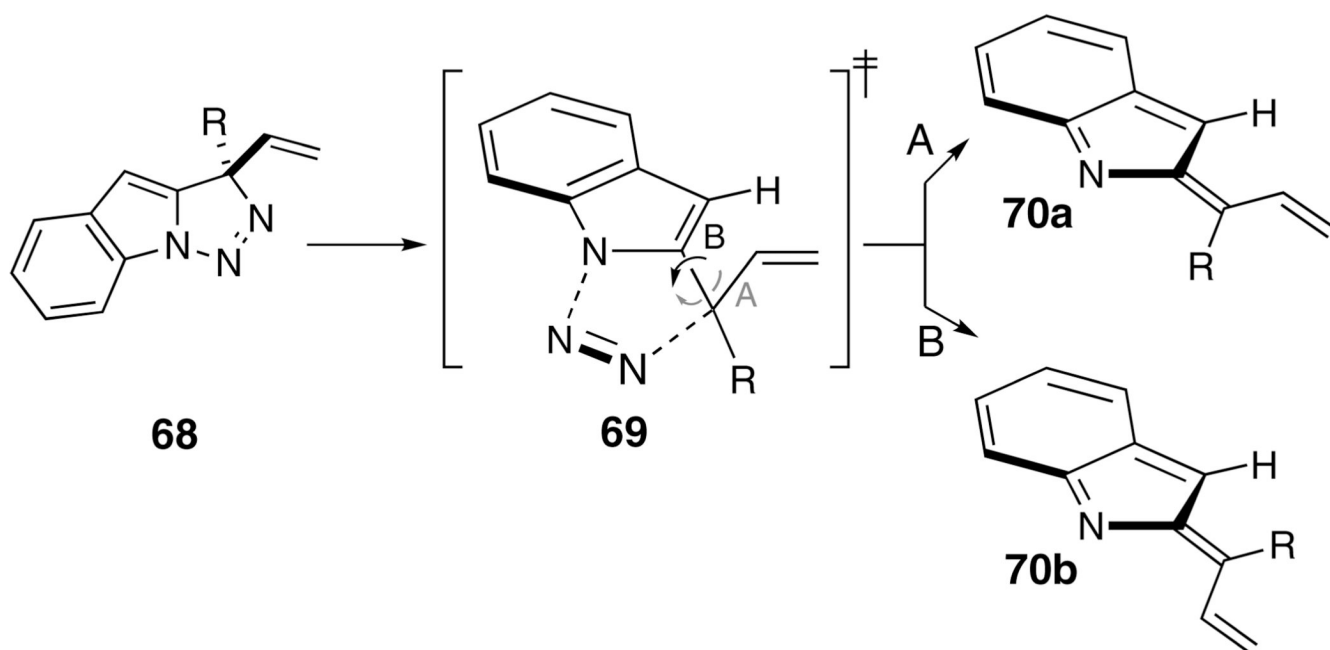
**SCHEME 6.**

Attempt To Synthesize a (Z)-Phenyl-Substituted 1-(2-Azidophenyl)-3-alkenylallene Substrate 63

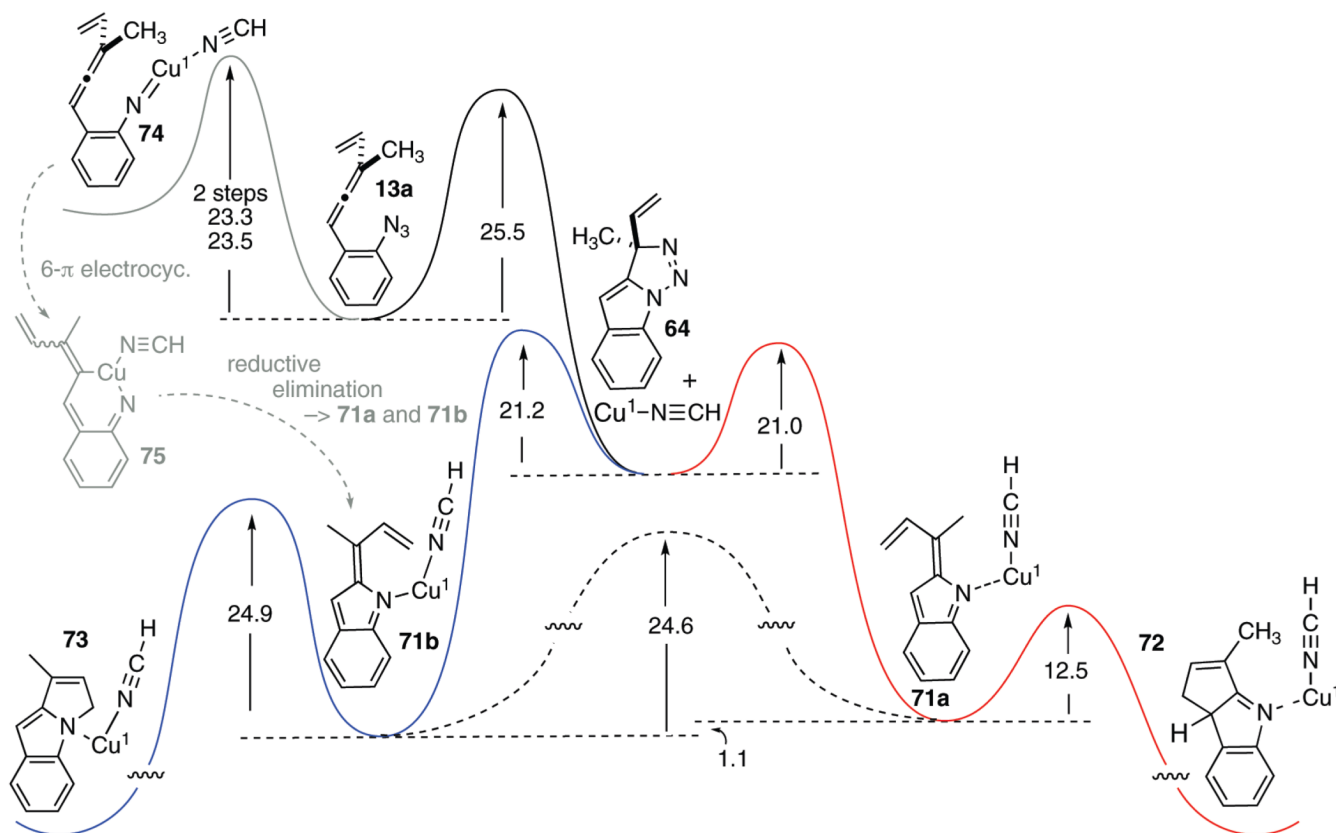
**SCHEME 7.**

Qualitative Representation of the Free Energy Profile for the Conversion of Azidoallene 13a into the C–C and C–N Cyclized Products 66 and 39a, Respectively^a

^aEnergies of ground-state structures and transition states were calculated using the B3LYP/6–311+G(d,p)//B3LYP/6–31G(d,p) functional. All energy values are in kcal/mol.



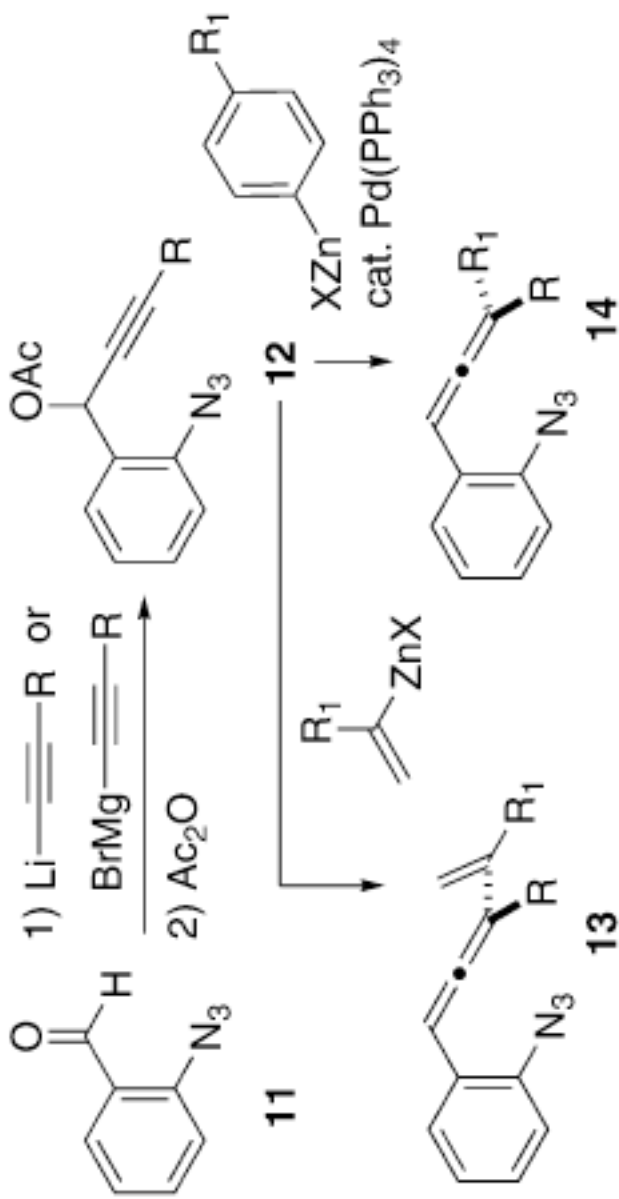
SCHEME 8.
Steric Interactions and Rotational Direction during Indolidene Formation



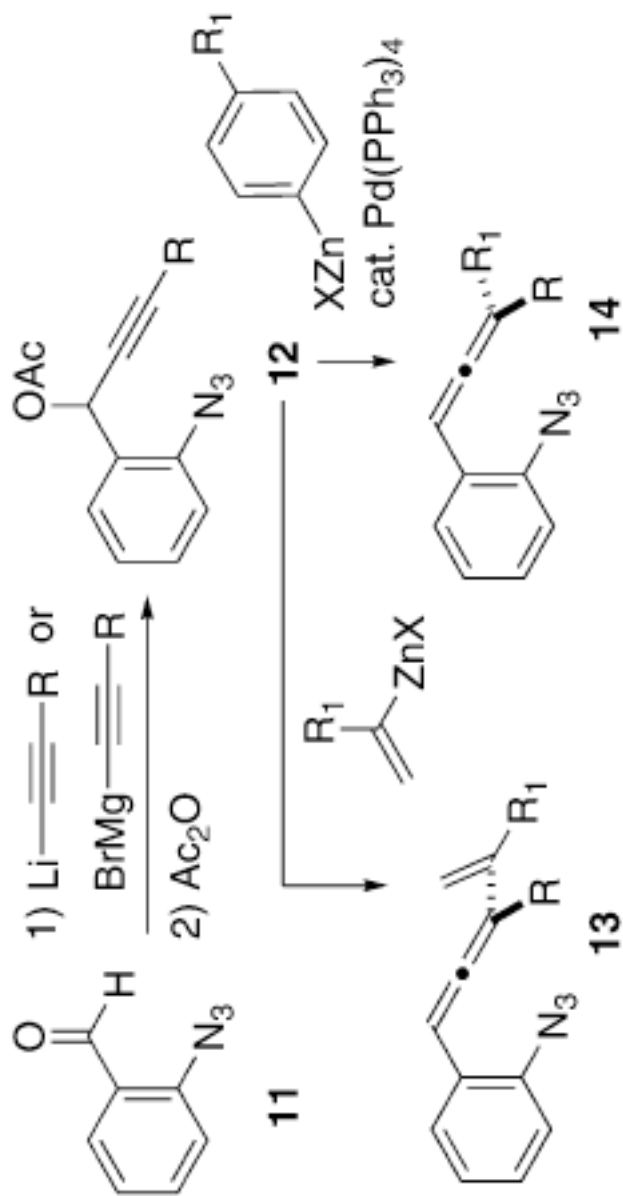
SCHEME 9.
Qualitative Representation of the Free Energy Profile for the Conversion of Allenyl Azide 13a into the C–C and C–N Cyclized Products 72 and 73, Respectively, in the Presence of Cu(I) •HCNa

^aEnergies of ground-state structures and transition states were calculated using the B3LYP/6–311+G(d,p)//B3LYP/6–31G(d,p) methodology.

TABLE 1

Simple Vinyl- and Phenyl-Substituted (*o*-Azidophenyl)allene Synthesis

entry	R	R ₁	yield of 12 ^a (%)	yield of 13 ^a (%)	yield of 14 ^a (%)
<i>a</i>	CH ₃	H	48	58	
<i>b</i>	CH ₂ OTBS	H	91	55	
<i>c</i>	(CH ₂) ₂ OTBS	H	73	57	
<i>d</i>	<i>t</i> -Bu	H	78	63	
<i>e</i>	CH ₃	Ph	48	67	
<i>f</i>	CH ₃	CH ₃	48	59	
<i>g</i>	Ph	CH ₃	79	69	
<i>h</i>	TMS	CH ₃	96	62	
<i>i</i>	H	CH ₃	82	49	
<i>j</i>	Ph	CH ₃ ^b	79		81



entry	R	R ₁	yield of 12 ^a (%)	yield of 13 ^a (%)	yield of 14 ^a (%)
<i>k</i>	CH ₃	<i>p</i> -(CH ₃ O)C ₆ H ₄	48		<i>c</i>
<i>l</i>	CH ₃	<i>m</i> -(CH ₃ O)C ₆ H ₄	48		<i>c</i>
<i>m</i>	CH ₃	<i>p</i> -FC ₆ H ₄	48		<i>c</i>

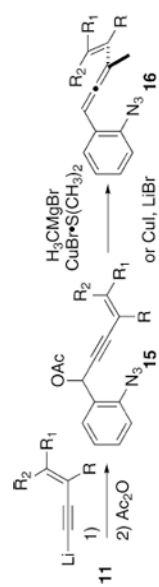
^a Isolated, chromatographically purified material.

^b CH₃MgBr/CuI/LiBr on **12j** (R = Ph).

^c The allenyls **14k–m** were not isolated but rather carried forward to the thermolysis reaction directly. See Scheme 5 for details.

TABLE 2

Synthesis of More Complex 1-(2-Azidophenyl)-3-alkenylallenes



entry	R	R ₁	R ₂	yield of 15 ^a (%)	yield of 16 ^a (%)
<i>a</i>	H	Ph	H	47	34
<i>b</i>	Ph	Ph	Ph	78	38
<i>c</i>	-(CH ₂) ₃ -		H	49	30
<i>d</i>	-(CH ₂) ₄ -		H	31	37

^a Isolated, chromatographically pure material.

TABLE 3

Preparation of Functionalized Cyclohexenyl-Substituted 1-(2-Azidophenyl)-3-(1-(1-cyclohexenyl)allenes)

Reaction scheme details:
 121 + CH_2R_2 , MgBr , CuI → Intermediate
 26 + $\text{cat. PdCl}_2(\text{PPh}_3)_2$, $\text{cat. CuI, Et}_3\text{N}$ → 27
 27 + Bu_4NF (93%) → 29
 29 + Dess-Martin oxidation (93%) → 30
 30 + Martin ox. (41%) → 28

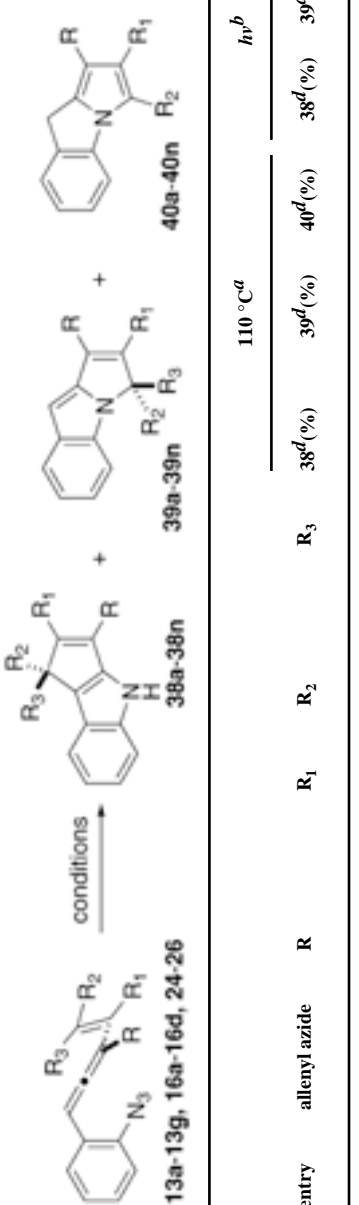
Substituent definitions:
 28a: $\text{R} = \text{OTBS}, \text{R}_1 = \text{H}$
 29: $\text{R} = \text{OH}, \text{R}_1 = \text{H}$
 30: $\text{R}, \text{R}_1 = \text{O}$

entry	R	R ₁	R ₂	yield of 27 ^a (%)	yield of 28 ^a (%)
<i>a</i>	TBS	H	H	79	92
<i>b</i>	TIPS	H	H	92	89
<i>c</i>	SEM	H	H	63	86
<i>d</i>	TBS	CN	H	76	81
<i>e</i>	TBS	H	TMS	79	85

^a Isolated, chromatographically pure material.

Cyclization Cascade of Substituted Vinyl (*o*-Azidophenyl)allenes To Furnish Indole and Pyrrole Products

TABLE 4



entry	allenyl azide	R	R ₁	R ₂	R ₃	110 °C ^a			hν ^b			hν/CuI ^c
						38 ^d (%)	39 ^d (%)	40 ^d (%)	38 ^d (%)	39 ^d (%)	40 ^d (%)	
<i>a</i>	13a	CH ₃	H	H	H	40			56	24	20	42
<i>b</i>	13c	(CH ₂) ₂ OTBS	H	H	H	52			43	24	16 ^f	36
<i>c</i>	13d	<i>t</i> -Bu	H	H	H	57			20	53	38	59
<i>d</i>	13b	CH ₂ OTBS	H	H	H	22			29	24	33	55
<i>e</i>	13e	CH ₃	Ph	H	H	40			30	44	31	67
<i>f</i>	13f	CH ₃	CH ₃	H	H	36			36	38	35	54
<i>g</i>	13g	Ph	CH ₃	H	H	47			39	23	11 ^{e,f}	69 ^f
<i>h</i>	23	CH ₃	H	CH ₂ OTBS	H	24	34		decomp			decomp
<i>i</i>	25	CH ₃	H	TBS	H	33			7	25	9	44 ^f
<i>j</i>	16a	CH ₃	H	Ph	H	(33) ^e	35		decomp			decomp
<i>k</i>	16c	CH ₃		-(CH ₂) ₃ -	H	(36) ^e	40		not examined			not examined
<i>l</i>	16d	CH ₃		-(CH ₂) ₄ -	H	36					51	54
<i>m</i>	24	CH ₃	CH ₃	(CH ₂) ₂ OTBS	H	7			40	(20) ^{e,g}	(40) ^{e,g}	42 ^g
<i>n</i>	16b	CH ₃	Ph	Ph	Ph	45	21			51	31	53

^a 100 mM in toluene.

^b 254 nm in CH₃CN (5 mM).

^c 254 nm in CH₃CN (5 mM), 150 mol % of CuI.

^d Isolated, chromatographically purified material.

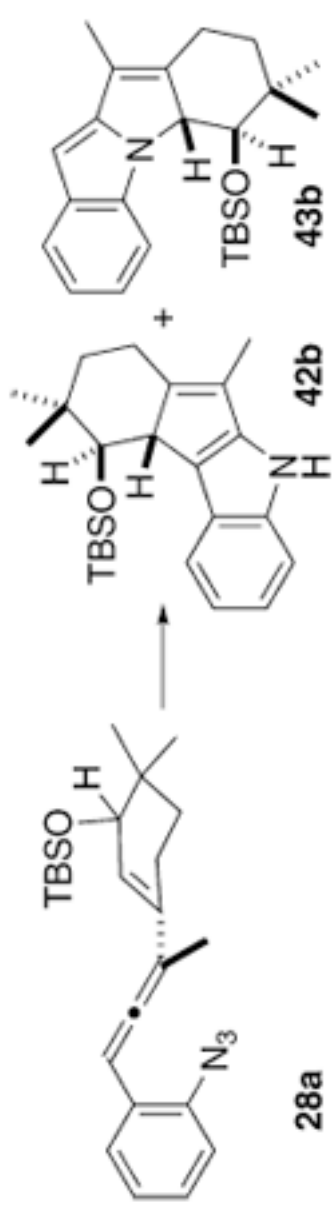
^e Not isolated; estimated by integration of the ¹H NMR spectrum of the crude reaction mixture.

^f Irradiated at 300 nm.

^g Irradiated at 350 nm.

TABLE 5

Discovery and Optimization of the CuI-Mediated Photochemical Cascade Cyclization of 29a into 42b

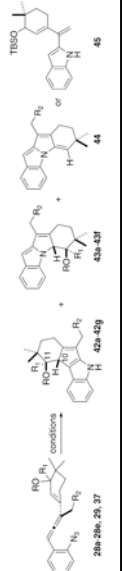


entry	irrad ^a (nm)	heat ^b (°C)	conditions	yield ^c (%)	42b/43b ratio ^d
<i>a</i>		110	no additives	80	1:1.6
<i>b</i>	254		no additives	67	1:1
<i>b</i>	254		excess CuI, LiBr, Mg powder	33	>10:1
<i>d</i>	254		LiBr (1 equiv)	68	1:1.1
<i>e</i>	254		Mg powder	(33) ^e	1:1.2
<i>f</i>	254		LiBr (1 equiv), CuI (0.05 equiv)	<i>f</i>	1:1.4
<i>g</i>	254		LiBr (1 equiv), CuI (1 equiv)	21	5.4:1
<i>h</i>	254		CuBr·SMe ₂ (1 equiv)	<i>f</i>	2.8:1
<i>i</i>	254		CuBr·SMe ₂ (0.25 equiv)	(17) ^e	1.6:1
<i>j</i>	254		Cu(OAc) ₂ (1 equiv)	<i>f</i>	5:1
<i>k</i>	254		CuI (0.5 equiv)	67	4:1
<i>l</i>	254		CuI (0.8 equiv)	72	6:1
<i>m</i>	254		CuI (1.2 equiv)	67	9:1
<i>n</i>	254		CuI (1.5 equiv)	70	10:1
<i>o</i>		110	CuI (1.5 equiv), 5 mM	75	1:1.6
<i>p</i>		110	CuI (1.5 equiv), 35 mM	66	3.5:1
<i>q</i>		110	CuI (1.5 equiv), 51 mM	65	5:1
<i>r</i>	254		[Rh(OAc) ₂] ₂ (1 equiv)	(48) ^e	1:1

- ^a Irradiated through a quartz vessel as a 5 mM CH₃CN solution of **28a**.
- ^b 100 mM solution in toluene, unless otherwise noted.
- ^c Isolated, chromatographically purified material. The N-cyclized material had undergone elimination to furnish the diene **44b** (see Table 6).
- ^d Ratio by integration of the ¹H NMR spectrum of the crude reaction mixture prior to chromatography.
- ^e Only the N-cyclized material was isolated; **42b** decomposed upon attempted chromatography.
- ^f Products were not isolated.

Cyclization Cascade of Substituted 1-(2-Azidophenyl)-3-cyclohexenylallenes To Furnish Indole Products

TABLE 6



entry	allenyl azide	R	R ₁	R ₂	110 °C ^d			hv ^b			hv/CuI ^c	
					42 ^d (%)	43 ^d (%)	44 ^d (%)	42 ^d (%)	43 ^d (%)	44 ^d (%)	42 ^d (%)	43 ^d (%)
<i>a</i>	29	H	H	H	34	25	21	24	60			
<i>b</i>	28a	TBS	H	H	34	25	33	34	62		8	
<i>c</i>	28b	TIPS	H	H		51	31	45	64		5	
<i>d</i>	28d	TBS	CN	H	27	48	27	43	62		7	
<i>e</i>	28	TBS	H	TMS		35	41 (45)	50	11 (45)		<i>f</i>	
<i>f</i>	28c	SEM	H	H	35	51	38	51	60			
<i>g</i>	37	TBS	H	OTBS		not examined			59			

^a 100 mM in toluene.^b 254 nm in CH₃CN (5 mM).^c 254 nm in CH₃CN (5 mM), 150 mol % CuI.^d Isolated, chromatographically purified material.^e Not isolated (unstable); estimated by integration of the ¹H NMR spectrum of the crude reaction mixture.^f A 1.6:1 ratio of **42e/45** was observed in the ¹H NMR spectrum of the crude reaction mixture; chromatographic purification of this CuI-mediated reaction gave irreproducible isolation results.

Cyclization Cascade with the H-Substituted- and TMS-Substituted 1-(2-Azidophenyl)-3-(2-propenyl)allene Substrates **13h** and **13i**, Respectively

TABLE 7

entry	allenyldiazide	conditions (CH ₃ CN)	51a/b ^a (%)	52a/b ^a (%)	53 ^a (%)	54 ^a (%)
<i>a</i>	13h	110 °C			53	23
<i>b</i>	13h	110 °C/150 mol % CuI	3		40	6
<i>c</i>	13h	254 nm	28	35	6	
<i>d</i>	13h	254 nm/150 mol % CuI	48		8	
<i>e</i>	13i	110 °C	12 ^b		9	
<i>f</i>	13i	254 nm		decomp		
<i>g</i>	13i	254 nm/150 mol % CuI		decomp		

^a Isolated, chromatographically purified material.

^b Observed in the ¹H NMR spectrum of the crude reaction mixture, but decomposed upon attempted chromatographic isolation.